1   # Novel inhibitors of *E. coli* lipoprotein diacylglyceryl transferase

2   # are insensitive to resistance caused by *lpp* deletion

3

4   Jingyu Diao[1], Rie Komura[2], Tatsuya Sano[2], Homer Pantua[1], Kelly M. Storek[1], Hiroko Inaba[2],

5   Haruhiko Ogawa[2], Cameron L. Noland[3], Yutian Peng[1], Susan L. Gloor[4†], Donghong Yan[5], Jing

6   Kang[5], Anand Kumar Katakam[6], Nicholas N. Nickerson[1†], Cary D. Austin[6], Jeremy Murray[3],

7   Steven T. Rutherford[1], Mike Reichelt[6], Yiming Xu[4], Min Xu[5], Hayato Yanagida[2], Junichi

8   Nishikawa[2], Patrick C Reid[2], Christian N. Cunningham[7, #] and Sharookh B. Kapadia[1, #]

9

10   Departments of Infectious Diseases[1], Structural Biology[3], Biochemical and Cellular

11   Pharmacology[4], Translational Immunology[5], Pathology[6] and Early Discovery Biochemistry[7],

12   Genentech, South San Francisco, CA 94080 USA

13   [2] Peptidream Inc., 3-25-23 Tonomachi, Kawasaki-ku, Kawasaki City, Kanagawa Prefecture,

14   JAPAN 210-0821

15   † Present address: S.L.G. - EpiCypher Inc., 6 Davis Drive Durham NC; N.N.N. - Hoffmann-La

16   Roche Ltd., 7070 Mississauga Road Mississauga, ON Canada

17

18   **Abstract word count:** 150

19   **[#] Corresponding authors**

20   Sharookh B. Kapadia (E-mail: kapadia.sharookh@gene.com)

21   Christian Cunningham (E-mail: cunningham.christian@gene.com)

Abstract

23   Lipoprotein diacylglyceryl transferase (Lgt) catalyzes the first step in the biogenesis of

24   Gram-negative bacterial lipoproteins which play crucial roles in bacterial growth and pathogenesis.

25   We demonstrate that Lgt depletion in a clinical uropathogenic *Escherichia coli* strain leads to

26   permeabilization of the outer membrane and increased sensitivity to serum killing and antibiotics.

27   Importantly, we identify the first ever described Lgt inhibitors that potently inhibit Lgt biochemical

28   activity *in vitro* and are bactericidal against wild-type *Acinetobacter baumannii* and *E. coli* strains.

29   Unlike inhibition of other steps in lipoprotein biosynthesis, deletion of the major outer membrane

30   lipoprotein, *lpp*, is not sufficient to rescue growth after Lgt depletion or provide resistance to Lgt

31   inhibitors. Our data validate Lgt as a novel druggable antibacterial target and suggest that inhibition

32   of Lgt may not be sensitive to one of the most common resistance mechanisms that invalidate

33   inhibitors of downstream steps of bacterial lipoprotein biosynthesis and transport.

34

35

36

37

38

39

40

41

42

43

Introduction

44

45   The cell envelope of a typical Gram-negative bacterium consists of two membranes: a

46   phospholipid inner membrane (IM) and an asymmetrical outer membrane (OM), the latter of which

47   is composed of a phospholipid inner leaflet and a lipopolysaccharide (LPS) outer leaflet. The IM

48   and OM are separated by the periplasm, which contains a peptidoglycan (PG) cell wall (reviewed in

49   detail in (Silhavy, Kahne, & Walker, 2010)). *E. coli* encodes >90 lipoproteins, many of which are

50   localized to the inner leaflet of the OM, but can also be exposed on the bacterial cell surface

51   (Cowles, Li, Semmelhack, Cristea, & Silhavy, 2011; Wilson & Bernstein, 2015). Bacterial

52   lipoproteins play critical roles in adhesion, nutrient uptake, antibiotic resistance, virulence, invasion

53   and immune evasion (Kovacs-Simon, Titball, & Michell, 2011), making the lipoprotein biosynthetic

54   and transport pathways attractive targets for novel antibacterial drug discovery.

55   Lipoprotein biosynthesis in Gram-negative bacteria is mediated by three IM localized

56   enzymes: Lgt, LspA and Lnt (Figure 1). All preprolipoproteins contain a signal peptide followed by

57   a conserved four amino acid sequence, [LVI][ASTVI][GAS]C, also known as a lipobox

58   (Schlesinger, 1992), and are secreted through the IM via the Sec or Tat pathways. After secretion

59   through the IM, Lgt catalyzes the attachment of a diacylglyceryl moiety from phosphatidylglycerol

60   to the thiol group of the conserved +1 position cysteine via a thioether bond (Sankaran & Wu,

61   1994). The second enzyme, prolipoprotein signal peptidase (LspA), is an aspartyl endopeptidase

62   which cleaves off the signal peptide N-terminal of the conserved diacylated +1 cysteine (M.

63   Tokunaga, Tokunaga, & Wu, 1982), and is the molecular target of the Gram-negative-specific

64   natural-product antibiotics globomycin and myxovirescin (Dev, Harvey, & Ray, 1985; Gerth,

65   Irschik, Reichenbach, & Trowitzsch, 1982; Olatunji et al., 2020; Xiao, Gerth, Müller, & Wall,

66   2012). In Gram-negative and high-GC Gram-positive bacteria, a third enzyme, lipoprotein N-acyl

3

67   transferase (Lnt), catalyzes the addition of a third acyl chain to the amino group of the N-terminal

68   cysteine via an amide linkage. Mature triacylated lipoproteins destined for the OM are extracted

69   from the IM by the LolCDE ATP-binding cassette (ABC) transporter and transported to the OM via

70   a periplasmic chaperone protein LolA and an OM lipoprotein LolB (Narita, 2011; Narita & Tokuda,

71   2010) (Figure 1).

72   **Figure 1: Lipoprotein biosynthesis and transport in Gram-negative bacteria**
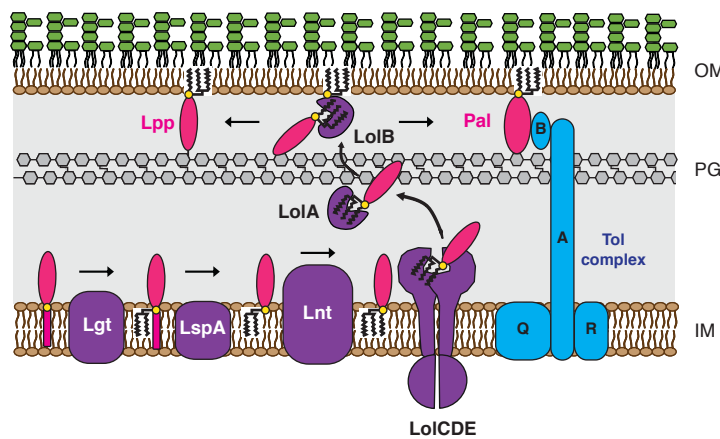
73

74   Two OM lipoproteins, Lpp (also known as Murein lipoprotein or Braun's lipoprotein) and

75   Pal (peptidoglycan-associated lipoprotein), mediate tethering of the PG layer to the OM in *E. coli*.

76   Lpp is a small ~8 kDa lipoprotein that is the most abundant OM protein in *E. coli* (~500,000

77   molecules per cell) and a third of all Lpp is covalently linked to PG (Cowles et al., 2011; Neidhardt,

78   1996). *E. coli* mutants deficient in Lpp exhibit increased OM permeability, leakage of periplasmic

79   components, increased outer membrane vesicle (OMV) release and increased sensitivity to

80   complement-mediated lysis (Diao et al., 2017; H. Suzuki et al., 1978; Yem & Wu, 1978).

81   Mislocalization and accumulation of PG-linked Lpp in the inner membrane upon inhibition of LspA

82   (Xiao et al., 2012; Zwiebel, Inukai, Nakamura, & Inouye, 1981) and LolCDE (McLeod et al., 2015;

83   Nickerson et al., 2018) is believed to lead to bacterial cell death (Narita & Tokuda, 2011; Robichon,

4

84   Vidal-Ingigliardi, & Pugsley, 2005; Yakushi, Tajima, Matsuyama, & Tokuda, 1997a). In addition

85   to Lpp, Pal binds PG and interacts with OmpA, Lpp and the Tol complex, and is crucial for

86   maintaining OM integrity in *E. coli* (Cascales, Bernadac, Gavioli, Lazzaroni, & Lloubes, 2002;

87   Clavel, Germon, Vianney, Portalier, & Lazzaroni, 1998; Leduc, Ishidate, Shakibai, & Rothfield,

88   1992; Mizuno, 1979). While non-natural product inhibitors of LspA and LolCDE have been

89   previously discovered (Kitamura, Owensby, Wall, & Wolan, 2018; McLeod et al., 2015), no

90   inhibitors of the first committed step in bacterial lipoprotein biosynthesis have been described.

91   Since many natural product antibiotics, including those that inhibit LspA, are cyclic (Igarashi, 2019;

92   Rossiter, Fletcher, & Wuest, 2017), we screened a macrocyclic peptide library to identify Lgt

93   inhibitors. In this study, we identify and characterize the first inhibitors of Lgt that inhibit growth

94   of wild-type *E. coli* and *A. baumannii* strains in addition to other OM-permeabilized Gram-negative

95   species. We demonstrate that, unlike inhibitors of LspA and LolCDE, treatment with Lgt inhibitors

96   does not lead to the significant accumulation of PG-linked Lpp forms in the IM and as such, are not

97   sensitive to resistance mediated by deletion of *lpp*.

98

99

100

101

102

103

104

105

106

Results

Modest depletion of Lgt leads to increased OM permeability and loss of bacterial viability is not rescued by deletion of *lpp*. Previous investigations into the role of Lgt in *E. coli* have focused on laboratory strains, specifically those lacking the O-antigen of LPS. Here, we engineered the uropathogenic *E. coli* clinical isolate CFT073 so that the only copy of *lgt* was under control of an arabinose-inducible promoter (CFT073Δ*lgt*), and hence requires arabinose for Lgt expression. As expected, genetic depletion of Lgt was lethal *in vitro* and growth was rescued after complementation with *E. coli lgt* (Figure 2a). *thyA*, the gene that encodes thymidylate synthase, is downstream of *lgt* and its ribosome binding site overlaps with the *lgt* stop codon. We confirmed that *thyA* expression, which is regulated by transcription from the *lgt* promoter and translational coupling (Gan et al., 1995), was unchanged after Lgt depletion (Figure 2-figure supplement 1a). Complementation with *lgt* from *Pseudomonas aeruginosa* PA14 or *A. baumannii* ATCC 17978 (51.6% and 48.6% sequence identity, respectively) was able to rescue viability (Figure 2a and Figure 2-figure supplement 1b). Overexpression of the *E. coli* genes encoding the downstream enzymes in lipoprotein biosynthesis (LspA, Lnt) and transport (LolCDE) did not rescue growth of CFT073Δ*lgt* in spite of detectable levels of LspA, Lnt and LolCDE (Figure 2-figure supplement 1c-g). While depletion of ~25% of Lgt was sufficient for bactericidal activity (Figure 2b and 2c), CFT073Δ*lgt* cells expressing as high as ~90% of normal levels of Lgt were significantly more sensitive to complement-mediated killing of the normally serum-resistant *E. coli* CFT073 and showed increased incorporation of SYTOX Green, a dye that normally does not penetrate an intact OM (Figure 2c-e). Depletion of Lgt also resulted in an expected increase in cell size (Figure 2f) and an Lpp-dependent IM contraction due to osmotic stress (Figure 2-figure supplement 2), as previously reported (Inukai et al., 1978a; Inukai, Nakajima, Osawa, Haneishi, & Arai, 1978b; Rojas

6

130   et al., 2018). Consistent with these results, partial depletion of Lgt that still allowed for normal

131   growth *in vitro* led to increased sensitivity to antibiotics that are normally excluded by the

132   impermeable Gram-negative OM (Table 1). Depletion of Lgt also resulted in significant attenuation

133   in a mouse *E. coli* bacteremic infection model (Figure 2g). Cumulatively, these data suggest that

134   Lgt could be a good antibiotic target since partial inhibition of Lgt may be sufficient to lead to

135   significant attenuation in growth and cellular morphology.

136

137 **Table 1**: Antibiotic sensitivity of WT CFT073 versus CFT073Δ*lgt* cells expressing wild-type (4%
138 Ara) or low (0.25% Ara) levels of Lgt
139
140

Antibiotic	MIC (µM)		
	WT CFT073	CFT073Δ*lgt*	
		Lgt $^{4\% \text{ Ara}}$	Lgt $^{0.25\% \text{ Ara}}$
Vancomycin (µM)	>100	>100	12.5
Rifamycin (µM)	6.3	6.3	0.8
Penicillin G (µM)	>50	>50	0.8
Oxacillin (µM)	>100	>100	12.5
Zeocin (µM)	12.5	12.5	0.8
Norfloxacin (µM)	0.4	0.6	0.2

141
142

143   Bactericidal activity of LspA and LolCDE inhibitors are sensitive to deletion of the gene

144   encoding the major OM lipoprotein, Lpp (McLeod et al., 2015; Zwiebel et al., 1981). To determine

145   if Lpp played a role in bacterial cell death after Lgt depletion, we constructed a *lgt* inducible

146   deletion strain in *E. coli* MG1655 with and without *lpp* (MG1655Δ*lgt* and MG1655Δ*lgt*Δ*lpp*) and

147   compared growth of these strains to *lspA* and *lolCDE* inducible deletion strains in the same

148   backgrounds. Expectedly, *lpp* deletion rescued the growth of the *lspA* and *lolCDE* inducible

149   deletions strains after depletion of LspA and LolCDE, respectively (Figure 2h). In contrast to LspA

7

150   and LolCDE depletion, the *lpp* mutant was more sensitive to Lgt depletion leading to a greater loss

151   of colony forming units (CFU) compared to that detected after Lgt depletion in cells expressing *lpp*.

152   Since the loss of *lpp* is a primary mechanism of resistance to inhibitors of LspA and

153   LolCDE thereby complicating their potential as antibacterial targets, identification of Lgt inhibitors

154   would uncover further biological understanding of this essential pathway, and potentially serve as

155   better starting chemical matter to develop novel antibiotics targeting lipoprotein biosynthesis that

156   are not sensitive to resistance mediated by *lpp* deletion.

157

158   **Identification and characterization of macrocyclic peptide inhibitors of Lgt.** Many natural

159   products or their derivatives account for a significant number of launched drugs and sine many of

160   them are cyclic in nature (Igarashi, 2019), we initially screened a macrocyclic peptide library to

161   identify specific and high affinity binders of Lgt. A genetically reprogrammed *in vitro* translation

162   system combined with mRNA affinity selection methods was used to generate large macrocycle

163   peptide libraries with sizes varying from 8-14 amino acids in length (Goto, Katoh, & Suga, 2011;

164   Ishizawa, Kawakami, Reid, & Murakami, 2013; Kashiwagi, Reid, & Inc, 2013) (Figure 3a). The

165   variable sequence (6-12 amino acids) of the macrocycle libraries encoded the random incorporation

166   of 11 natural amino acids (Ser, Tyr, Trp, Leu, Pro, His, Arg, Asn, Val, Asp, and Gly) and 5 non-

167   natural amino acids (Figure 3b). The screening of the libraries is schematically depicted in Figure

168   3c. Lgt-biotin was solubilized in 0.02% n-Dodecyl β-D-maltoside (DDM), immobilized on

169   streptavidin magnetic beads and incubated with the macrocyclic library. Iterative rounds of affinity

170   selection were performed to identify Lgt-binding macrocycles. After five rounds of enrichment,

171

Inhibition of Lgt in Gram-negative bacteria

172   **Figure 2: Lgt is essential for *in vitro* growth, membrane integrity, serum resistance and**

173   **virulence**

174

175
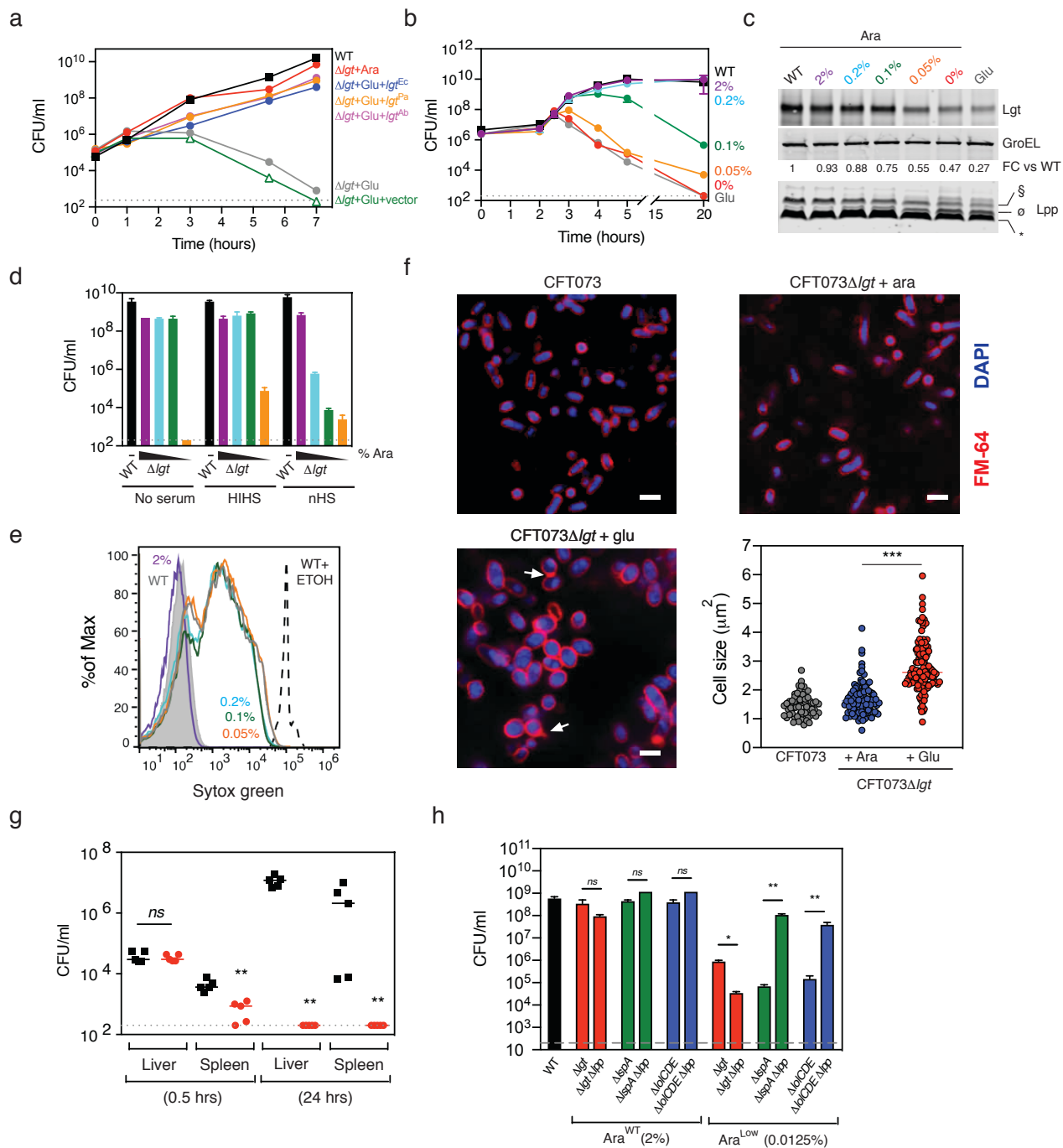
176   two additional rounds of off-rate selections were performed by increasing the wash stringency

177   before high affinity binders were eluted. Hit macrocycles were identified using next generation

178   sequencing on the last four rounds of selection followed by a frequency analysis calculation. Three

179   macrocycles were identified from these screens, **508**, **692**, and **693** (Figure 3-figure supplement 1),

180   with a frequency enrichment in the final round of selection of 4.1%, 19.4%, and 10.1%,

181   respectively, as measured by NGS. **508** contains 8 amino acids with a molecular weight (MW) of

182   1264.49 Da. **692** and **693** each contain 7 amino acids and are related to one another with a charge

183   swap at position 2, and have MWs of 1428.66 and 1259.55 respectively. The calculated LogPs

184   (cLogP), which is the logarithm of the compounds partition coefficient between n-octanol and water

185   and a measure of a molecule's hydrophilicity, were 4, 1.8 and 1.7 for **508**, **692** and **693**,

186   respectively. **692** was synthesized with a Gly off of the C-terminus and renamed G9066 (Figure

187   3d). During re-synthesis, both **508** and **693** were synthesized with a Gly-Lys-Lys tail off of the C-

188   terminus to aide in solubility of these macrocycles and were renamed G2823 and G2824,

189   respectively (Figure 3d).

190   We then tested the ability of G9066, G2823 and G2824 to inhibit *E. coli* Lgt enzymatic

191   activity *in vitro* by measuring the release of glycerol phosphate which is a by-product of the Lgt-

192   catalyzed transfer of diacylglyceryl from phosphatidylglycerol to a peptide substrate via formation

193   of a thioether bond. The peptide substrate was derived from the Pal lipoprotein (Pal-IAAC, where

194   C is the conserved cysteine that is modified by Lgt). While glycerol-1-phosphate (G1P) is the

195   expected by-product of the Lgt enzymatic activity (Sankaran & Wu, 1994), the

196   phosphatidylglycerol substrate used in our biochemical assay contains a racemic glycerol moiety at

197   the end of phosphatidyl group, and hence both G1P and glycerol-3-phosphate (G3P) are released

198   from phosphatidylglycerol as Lgt catalyzes the reaction (Figure 3e). The detection of G3P is based

10

Inhibition of Lgt in Gram-negative bacteria

199   **Figure 3: Identification of Lgt inhibitors**
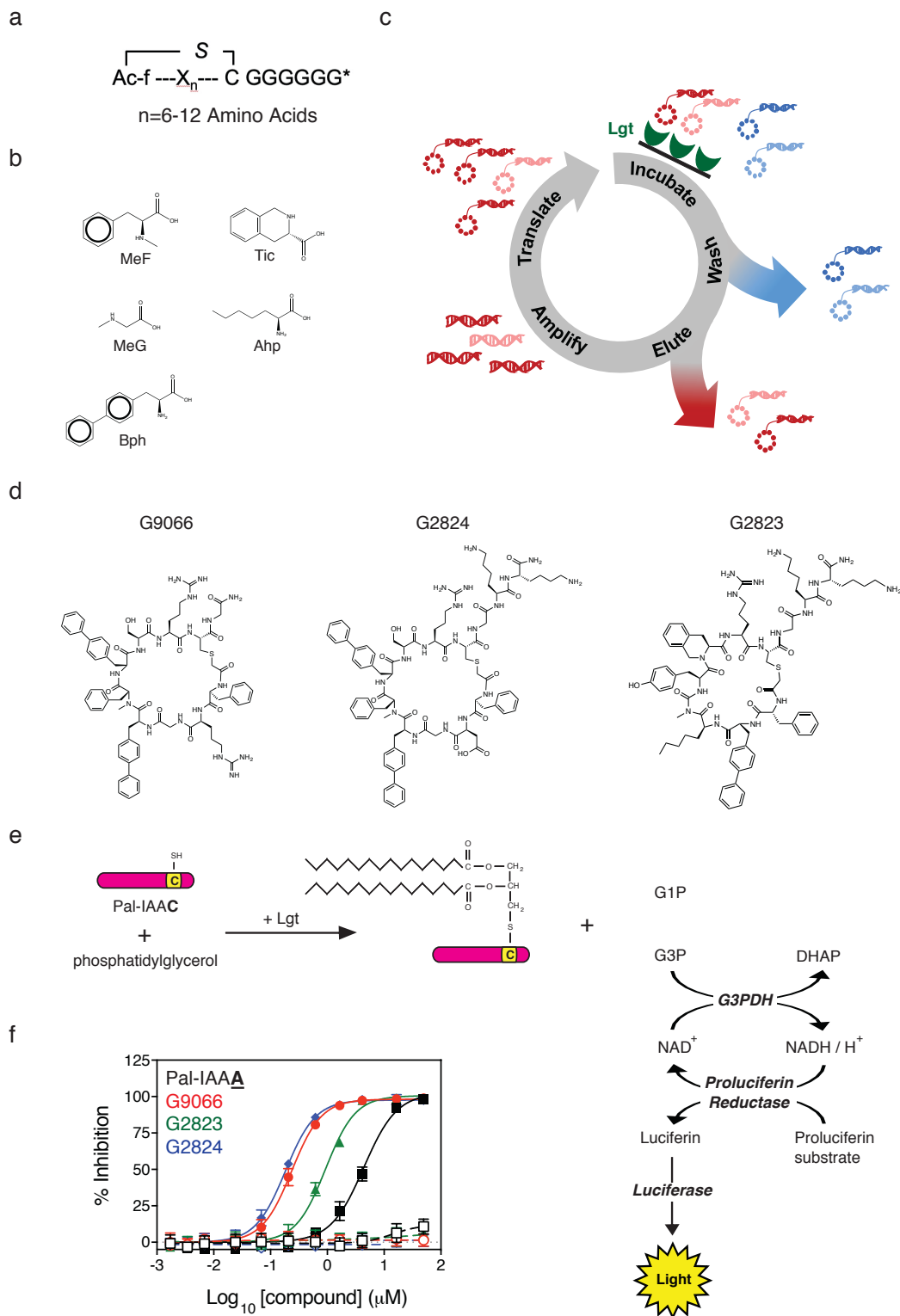
201   on a coupled luciferase reaction which is described in more detail in the Methods and in Figure 3e.

202   G9066, G2823 and G2824 potently inhibited Lgt biochemical activity (IC_{50}=0.24 μM, 0.93 μM and

203   0.18 μM, respectively) (Figure 3f). In comparison, a mutant Pal peptide substrate with the

204   conserved cysteine mutated to alanine (Pal-IAA**A**), which cannot get modified and acts as a Lgt-

205   binding nonreactive, substrate-based competitive inhibitor, inhibited Lgt with an IC_{50}=4.4 μM

206   (Figure 3f). When tested against bacterial cells in minimal inhibitory concentration (MIC) growth

207   assays, G9066 and G2824 inhibited growth of WT *A. baumannii* 19606 with a MIC = 37.5 μM.

208   G2823 and G2824 inhibited *E. coli* MG1655 growth with a MIC = 50 μM (Table 2). OM

209   permeabilization either genetically (*imp*4213 mutation) or chemically (EDTA treatment) of all

210   **Table 2: Growth inhibition of a panel of bacterial strains and eukaryotic cells by Lgti, LspAi**

211   **and LolCDEi**

Bacteria	Strain	Lgti			LspAi	LolCDEi	Vancomycin
		G9066	G2823	G2824	GBM	C1	
E. coli (MIC, μM)	MG1655	>100	50	50	25	>100	>100
	MG1655 + EDTA	3.1	3.1	3.1	0.8	3.1	3.1
	MG1655Δ*lpp* + EDTA	3.1	3.1	3.1	12.5	12.5	0.8
	CFT073	100	83.3	92	29.2	50	>100
	CFT073Δ*lpp*	31.3	25	62.5	>100	>100	>100
	CFT073 + EDTA	3.1	4.2	3.1	1.1	2.1	0.8
	CFT073Δ*lpp* + EDTA	1.6	3.1	2.3	4.7	9.4	0..8
	CFT073*imp*4213	5.7	8.4	8.4	0.5	2.1	0.6
	CFT073*imp*4213Δ*lpp*	6.8	9.4	8.9	11.5	17.7	0.7
A. baumannii (MIC, μM)	19606	37.5	100	37.5	25	100	>100
	19606 + EDTA	3.1	4.7	6.3	0.6	12.5	0.2
P. aeruginosa (MIC, μM)	PA14	>100	>100	>100	>100	>100	>100
	PA14*imp*4213	6.3	6.3	6.3	50	>100	12.5
	PA14 + EDTA	6.3	6.3	6.3	50	50	6.3
S. aureus (MIC, μM)	USA300	6.3	>100	>100	>100	>100	0.4
Mammalian cytotoxicity (EC_{50}, μM) [§]	HepG2	> 100	> 100	> 100	> 100	> 100	> 100
	Hela	> 100	> 100	> 100	> 100	> 100	> 100
	293T	> 100	> 100	> 100	> 100	> 100	> 100

212 * All *E. coli* MIC values represent averages from at least four independent experiments each performed in duplicate.
213 For other bacterial strains, MIC values represent averages from two independent experiments each performed in
214 duplicate
215 [s] Mammalian cytotoxicity values are representative of three independent replicates
216

217

218 Gram-negative strains, including *P. aeruginosa* PA14 and *A. baumannii* 19606, led to growth

219 inhibition (Table 2). Interestingly, *lpp* deletion in either CFT073*imp*4213 or CFT073 treated with

220 EDTA did not lead to increases in G9066, G2823 or G2824 MIC, unlike that seen with inhibitors of

221 LspA and LolCDE (Table 2). In fact, *lpp* deletion in WT CFT073 cells led to a modest increase in

222 G9066, G2823 and G2824 potency. G2823 and G2824 showed minimal non-specific activity

223 against eukaryotic cells and the Gram-positive *Staphylococcus aureus* strain USA300, consistent

224 with data demonstrating *lgt* is dispensable for Gram-positive bacterial growth *in vitro* (Stoll,

225 Dengjel, Nerz, & Götz, 2005). In contrast, G9066 inhibited growth of USA300 to a greater extent

226 suggesting G9066 may have additional targets or non-specific cellular effects. Given G9066 and

227 G2824 are very similar, we decided to focus the remainder of this study on G2823 and G2824

228 (hereafter referred to as Lgti).

229

230 **G2823 and G2824 specifically inhibit Lgt in *E. coli***

231 While the Lgti inhibited both Lgt enzymatic function and bacterial growth, it was unclear whether

232 inhibition of bacterial cell growth was mediated by specific inhibition of Lgt function. We were

233 unable to raise on-target resistant mutants to Lgti, and hence multiple experimental approaches were

234 undertaken to determine if inhibition of bacterial growth was indeed Lgt-dependent. As the

235 accumulation of Lpp intermediates detected by Western blot analyses has been successfully used to

236   verify inhibition or deletion of specific enzymes involved in lipoprotein biosynthesis or transport

237   (Narita & Tokuda, 2011; Nickerson et al., 2018), we asked if Lgt treatment led to the accumulation

238   of pro-Lpp, the substrate of Lgt. We initially sought to verify the various Lpp forms by leveraging

239   a previously described protocol using SDS fractionation (Diao et al., 2017; Nakae, Ishii, &

240   Tokunaga, 1979; Whitfield, Hancock, & Costerton, 1983). Lysozyme was added to allow for the

241   identification of PG-linked Lpp forms, as previously demonstrated (M. Suzuki, Hara, & Matsumoto,

242   2002). CFT073 cell lysates were centrifuged to separate the SDS-insoluble PG-associated proteins

243   (PAP) and SDS-soluble non-PG-associated proteins (non-PAP) (Figure 4a) and Lpp were detected

244   by Western blot analysis. As expected, the fastest migrating form representing the triacylated

245   mature form of Lpp (*) was enriched in the non-PAP fraction and the PG-linked Lpp forms (†) were

246   enriched in the PAP fraction (Figure 4b). We also detected a form corresponding to the PG-linked

247   diacylglyceryl modified pro-Lpp (DGPLP, §), as previously reported (M. Suzuki et al., 2002). We

248   then asked if we could detect pro-Lpp in total cell lysates after Lgt depletion and used the *lspA* and

249   *lolCDE* inducible deletion strains as controls. We confirmed that specific depletion of Lgt led to the

250   accumulation of the unmodified pro-Lpp (UPLP, ø), (Figure 4c), consistent with previous results

251   (Pailler, Aucher, Pires, & Buddelmeijer, 2012). While depletion of LspA led to the accumulation of

252   DGPLP (§) and other PG-linked Lpp forms (†), depletion of LolCDE did not change the SDS-

253   PAGE migration of Lpp as LolCDE is only critical for transport to the OM and does not affect

254   lipoprotein biosynthesis (Figure 4c). These results now allowed us to determine whether the Lgti

255   identified in this study inhibited Lgt in bacterial cells.

256   As the Lgti have only moderate activity against WT bacterial strains, we performed

257   mechanistic studies with Lgti in the CFT073 cells containing the *imp*4213 allele in *lptD*

258   (CFT073*imp*4213), which leads to permeabilization of the OM (Ruiz, Falcone, Kahne, & Silhavy,

259   2005). Given the high expression of Lpp, we engineered CFT073*imp*4213 cells to only express an

260   arabinose inducible *lpp* (CFT073*imp*4213Δ*lpp:lpp*[Ara]) to minimize the background from pre-formed

261   Lpp. *lpp* gene expression was induced prior to treatment with sub-MIC levels of Lgti and led to an

262   accumulation of UPLP (ø, Figure 4d), similar to what was observed with the CFT073Δ*lgt* strain

263   (Figure 4c), and a concurrent decrease in the triacylated mature Lpp form (*, Figure 4d). While

264   treatment with globomycin (LspAi) led to an accumulation of DGPLP and other PG-linked Lpp

265   forms, treatment of cells with the AstraZeneca LolCDE inhibitor C1 (LolCDEi) (McLeod et al.,

266   2015) did not lead to significant accumulation of Lpp, which is consistent with our data using the

267   inducible deletion strains as well as published results (Narita & Tokuda, 2011; Nickerson et al.,

268   2018). These data demonstrate that the Lgti identified in this study inhibit the generation of mature

269   triacylated Lpp and lead to the accumulation of UPLP, which is the substrate of Lgt.

270   Lgt on-target activity was further confirmed using two additional methods. First, Lgti

271   treatment also led to the expected OM blebbing and increase in cell size (Figure 4e and 4f), the

272   former of which was previously demonstrated in a Pal-deficient *E. coli* strain (Kowata, Tochigi,

273   Kusano, & Kojima, 2016). Second, we asked whether cells expressing reduced levels of Lgt would

274   be specifically sensitized to Lgti compared to the other inhibitors. To test this hypothesis, we

275   utilized CRISPRi technology to decrease gene expression of the enzymes involved in lipoprotein

276   biosynthesis and transport. BW25113 cells containing plasmids expressing dCas9 and guide RNAs

277   (gRNAs) specific to *lgt*, *lspA*, *lolC* were treated with Lgti, LspAi and LolCDEi and bacterial growth

278   was measured. Scrambled (scr) and a *folA*-specific gRNAs were used as negative controls. Levels

279   of downregulation of target gene expression (Figure 4-figure supplement 1) were consistent with

280   published reports for CRISPRi in bacterial cells (Rousset et al., 2018). Decreased expression of *lgt*

281   specifically sensitized cells to Lgti but not LspAi and LolCDEi (Figure 4g and

282   **Figure 4: Lgti inhibit Lgt enzymatic activity in bacterial cells.**

283

284
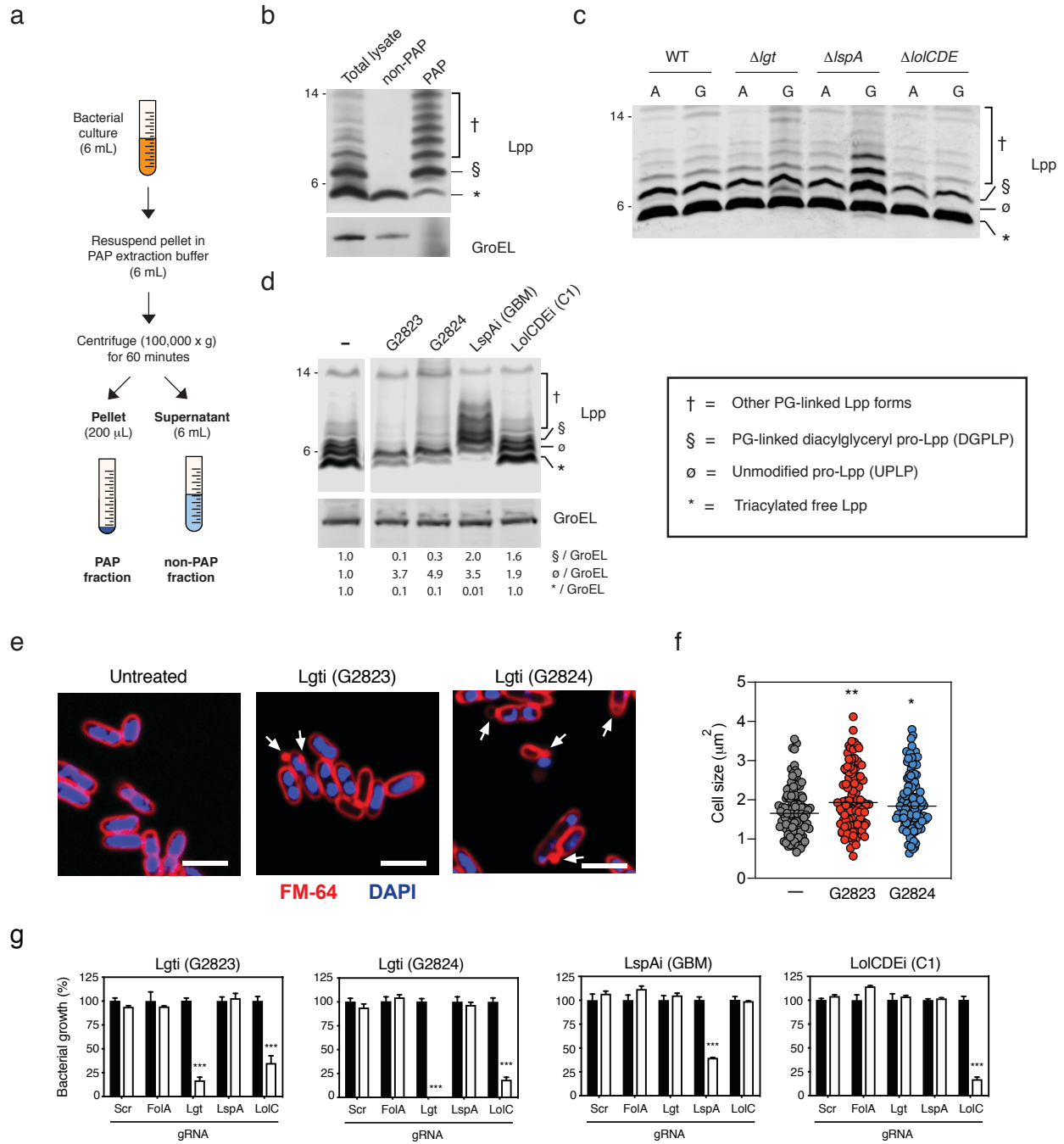
285   Figure 4-figure supplement 2). As expected, decreased expression of *lspA* and *lolC* specifically led

286   to enhanced growth inhibition by LspAi and LolCDEi compounds, respectively (Figure 4g and

287   Figure 4-figure supplement 2a,b). Decreased *lolC* expression also sensitized cells to Lgti (Figure

288   4g) and, at higher concentrations, LspAi (Figure 4-figure supplement 2d), but we confirmed that

289   previously identified LolCDEi-resistant mutants were not cross-resistant to Lgti (Supplemental

290   Table 1). Cumulatively, our data demonstrate that the novel Lgt-binding macrocycles G2823 and

291   G2824 interfere with Lgt activity leading to inhibition of *E. coli* growth.

292

293   **Antibacterial activity of Lgti is not sensitive to *lpp* deletion.**

294   Our data with the inducible deletion strains (Figure 2h) suggested that the mechanism of cell death

295   upon Lgt depletion is independent of Lpp (Figure 2h), distinguishing it from the mechanism of cell

296   death after depletion of enzymes involved in later steps of lipoprotein biosynthesis. Since the Lgti

297   identified in this study now allowed us to pharmacologically intervene at this step in the pathway,

298   we compared the bactericidal activity of Lgti with that of LspAi and LolCDEi. We treated

299   CFT073*imp*4213 and CFT073*imp*4213Δ*lpp* cells with Lgti (G2824), LspAi (GBM) and LolCDEi

300   (C1) at 2×MIC of the respective inhibitors against CFT073*imp*4213 and enumerated viable CFU

301   counts. Consistent with our data using the inducible deletion strains, *lpp* deletion did not protect

302   cells from Lgti (Figure 5a). In fact, the rate of CFU loss after Lgti treatment was more rapid in *lpp*-

303   deleted cells, which is consistent with our data using the CFT073Δ*lgt* cells (Figure 2h) and indicates

304   a protective role for Lpp when targeting Lgt. As expected, inhibition of bacterial growth by LspAi

305   and LolCDEi was lost in the absence of *lpp* (Figure 5b and 5c). In contrast, vancomycin showed

306   equivalent killing of CFT073*imp*4213 and CFT073*imp*4213Δ*lpp* at 5 hours post treatment (Figure

307   5d). These data confirm that *lpp* deletion is not a mechanism of resistance to Lgti, and in fact

308   protects cells against depletion or inhibition of Lgti.

309

310   **Figure 5: *lpp* deletion does not rescue growth after Lgti treatment**

311
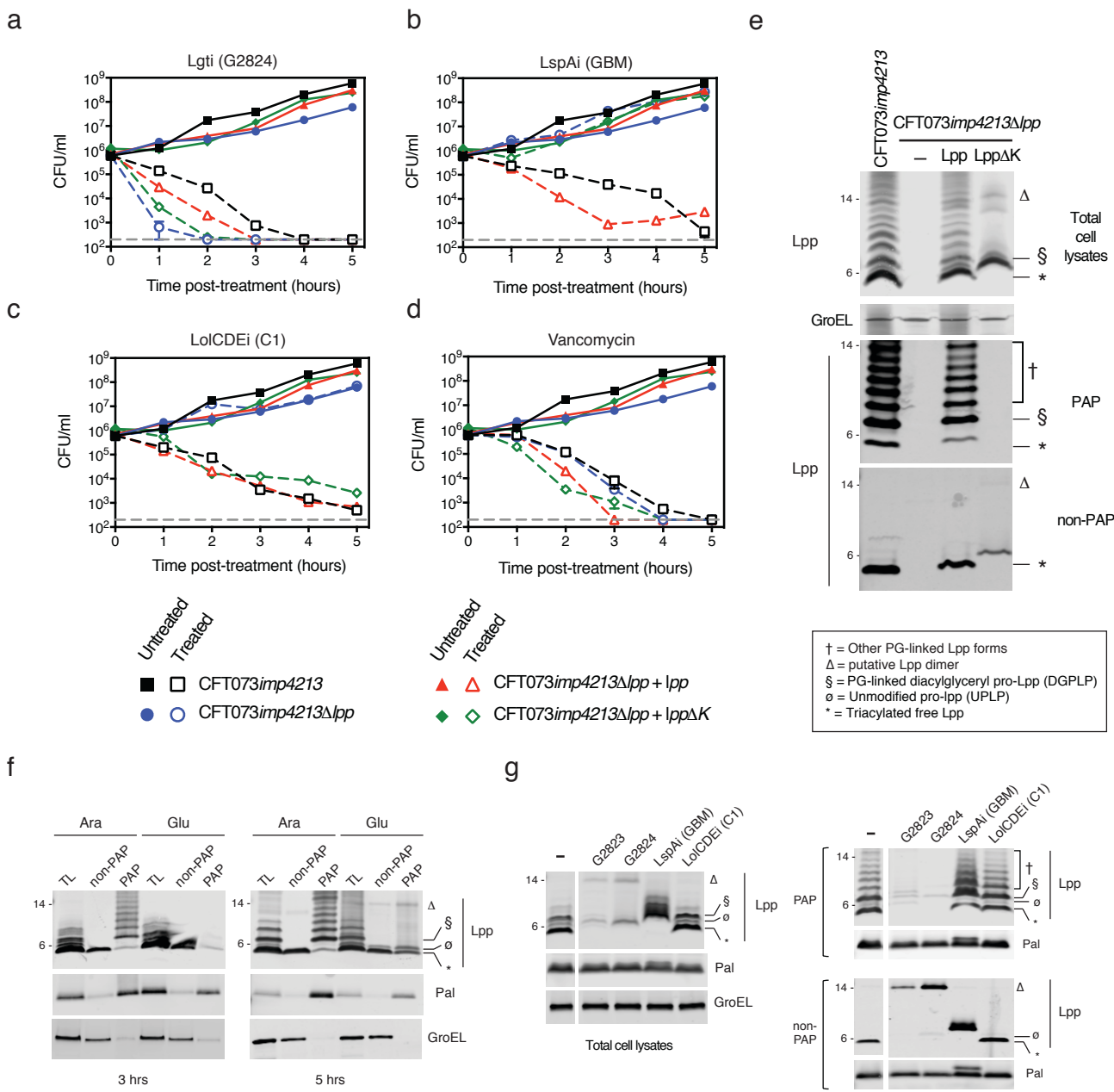
312   To determine if PG-linkage of Lpp plays a role in protection against Lgti, we treated

313 CFT073*imp*4213Δ*lpp* cells complemented with either WT *lpp* or a mutant form that is unable to

314 covalently link to PG (*lpp*Δ*K*). Using the previously described SDS fraction protocol, we

315 confirmed that while WT Lpp localized to both PAP and non-PAP fractions, the LppΔK mutant was

316 only detected in the non-PAP fraction (Figure 5e). As we noted earlier, PG-linked DGPLP (§) and

317 other PG-linked Lpp forms (†) were primarily detectable in cell lysates and PAP fraction (Figure

318 5e). While complementation of CFT073*imp*4213Δ*lpp* with WT *lpp* led to increased bactericidal

319 activity of LspAi and LolCDEi, bactericidal activity of Lgti and LolCDEi in cells deleted for *lpp* or

320 those only expressing LppΔK was comparable (Figure 5a-c). These data suggest that while PG-

321 linked Lpp is toxic to cells after treatment with LspAi, it functions as a protective mechanism

322 against Lgti. Furthermore, accumulation of PG-linked Lpp does not fully explain the bactericidal

323 activity of LolCDEi.

324

325 Lgt depletion or inhibition leads to decreased PG-association of Lpp and Pal.

326 Unlike with inhibitors of LspA (Yakushi, Tajima, Matsuyama, & Tokuda, 1997a) and LolCDE

327 (Nickerson et al., 2018), Lpp protects cells from Lgti suggesting that the PG-linkage state and/or

328 localization of Lpp must differ after treatment with Lgti. Using SDS fractionation to enrich for PG-

329 associated proteins in the CFT073Δ*lgt* inducible deletion strain, we find that while Lgt depletion

330 leads to a significant loss of DGPLP and other PG-linked Lpp forms in the PAP fractions, there is a

331 modest accumulation of UPLP in the PAP fraction (Figure 5f). Lgt depletion also led to decreased

332 PG-associated Pal, although the difference between pro-Pal and mature Pal forms was difficult to

333 distinguish by SDS-PAGE due to larger size of Pal compared to Lpp. We then tested if Lgti

334   treatment also led to a similar loss of PG-association of Lpp and Pal. As before, we used cells

335   expressing an inducible form of *lpp* (CFT073*imp*4213Δ*lpp:lpp*^{Ara}) and find that Lgti treatment leads

336   to decreased PG-associated DGPLP and other PG-linked Lpp forms Lpp (Figure 5g). In addition,

337   we also detect a modest decrease in PG-associated Pal (Figure 5g). As expected, LspAi treatment

338   led to the accumulation of PG-linked DGPLP (§) and other PG-linked Lpp forms (†). These data

339   suggest that the accumulated UPLP after Lgt inhibition is either not significantly linked to PG or

340   does not accumulate to levels needed to induce cell death. To address the first question, we

341   engineered cells to only express a mutant of Lpp that has the conserved cysteine modified

342   (CFT073*imp*4213Δ*lpp:lpp*^{C21A}) and asked if this form was PG-linked. Lpp^{C21A} cannot be modified

343   by Lgt and represents the pro-Lpp substrate of Lgt. While complementation of

344   CFT073*imp*4213Δ*lpp* with WT Lpp led to normal PG-linkage, CFT073*imp*4213Δ*lpp:lpp*^{C21A} cells

345   showed a significantly less PG-association of Lpp (Figure 5-figure supplement 1). Cumulatively,

346   these data demonstrate that inhibition of Lgt leads to decreased PG-association of Lpp, which could

347   explain why deletion of *lpp* does not lead to resistance to Lgti.

348

349   **Inhibition of Lgt does not lead to significant accumulation of PG-linked Lpp in the IM**

350   We then asked if membrane localization of Lpp, other OM lipoproteins and OMPs were affected by

351   Lgti. We utilized sucrose gradient centrifugation to separate *E. coli* IM and OM and measured

352   levels of OM lipoproteins (Lpp, Pal, BamD) and OMPs (BamA, OmpA) by Western blot analyses.

353   Sucrose gradient centrifugation of CFT073*imp*4213 cells membranes led to the efficient separation

354   of IM and OM, as measured by MsbA and OmpA expression, respectively (Figure 6a). In

355   comparison to untreated cells, Lgti treatment led to significant reductions of Lpp in the OM (Figure

20

Figure 6: Inhibition of Lgt leads to depletion of essential OM lipoproteins and OMPs and

minimal IM accumulation of PG-linked DGPLP
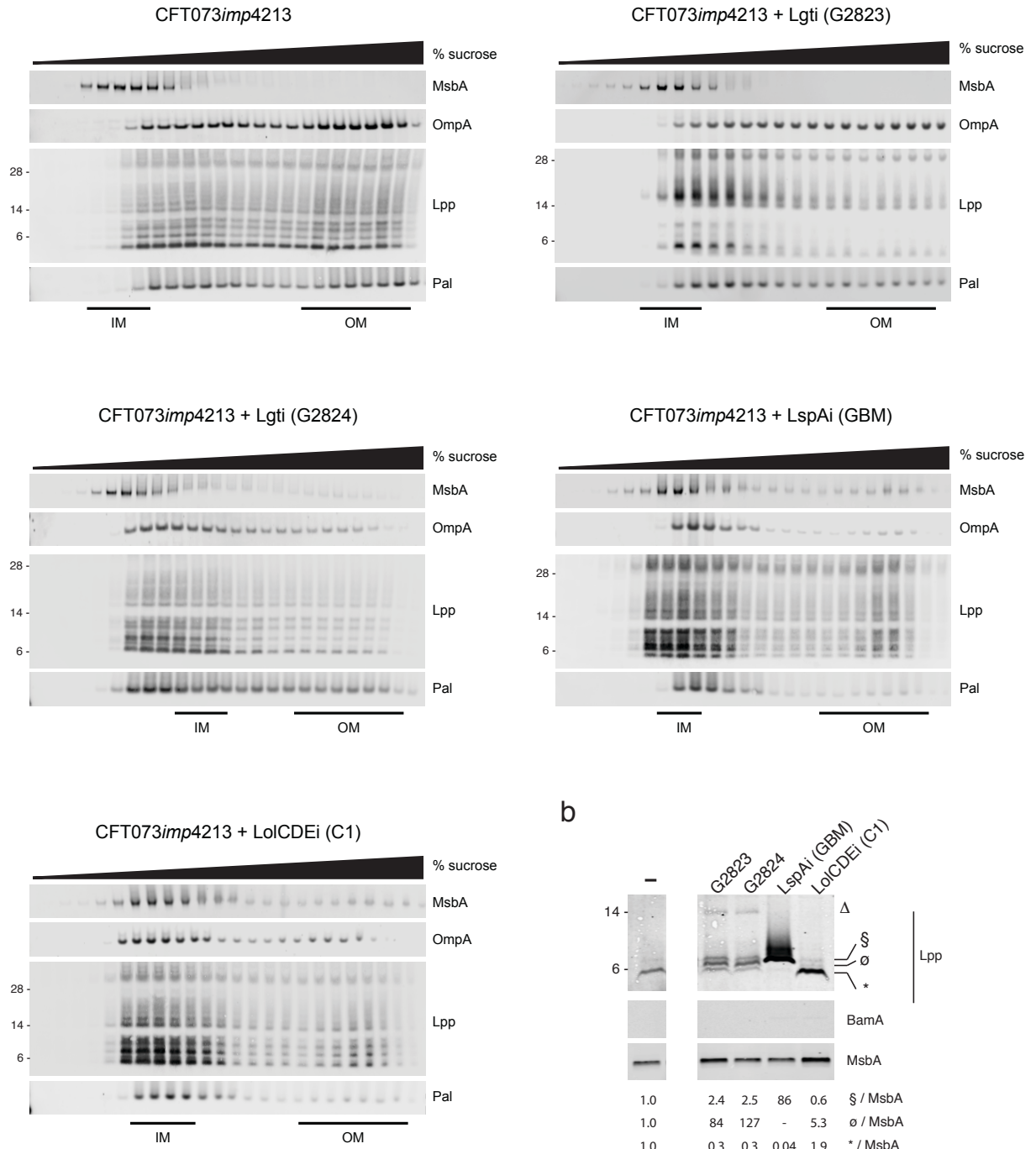
a

360   6a). Although Lgti treatment led to accumulation of Lpp in the IM, the levels were significantly

361   lower than that seen with LspAi and LolCDEi. All the inhibitors led to decreased OM localization

362   of other lipoproteins, Pal and BamD, as well as the OM β-barrel proteins BamA and OmpA (Figure

363   6 and Figure 6 – figure supplement 1). These results are not totally unexpected given OmpA

364   insertion into the OM requires BamA function, which itself requires other Bam lipoproteins,

365   including BamD, for proper OM localization. These results suggest that while Lgti are similar to

366   LspAi and LolCDEi in their effects on Pal and other lipoproteins involved in OM biogenesis

367   pathways, they differ from LspAi and LolCDEi in that they do not lead to significant accumulation

368   of Lpp in the IM supporting our data that *lpp* deletion does not play major role in resistance to Lgti.

369   In addition to sucrose gradient centrifugation, we also treated cells with sarkosyl that

370   specifically solubilizes the IM and has been used for IM proteomic analyses in multiple Gram-

371   negative bacteria (Ferrer-Navarro, Ballesté-Delpierre, Vila, & Fàbrega, 2016; Filip, Fletcher, Wulff,

372   & Earhart, 1973; Hobb, Fields, Burns, & Thompson, 2009; Jabbour et al., 2010). Compared to

373   untreated cells, treatment with Lgti led to a ~84 to 127-fold increase in levels of UPLP in the IM. In

374   contrast, DGPLP levels in the IM increased by a modest ~2.5-fold in comparison to LspAi

375   treatment, which results in a ~86-fold increase of DGPLP in the IM (Figure 6b). These results

376   confirm that Lgti treatment leads to minimal accumulation of inefficiently PG-linked UPLP in the

377   IM, but no significant accumulation of other PG-linked Lpp forms, including the DGPLP.

378

379

380

381 **Discussion**

382   Lipoprotein biosynthesis is a critical pathway involved in the biogenesis and maintenance of the

383   Gram-negative bacterial OM, and disruption of any step in this pathway leads to loss of cell

384   viability. Lpp maintains the integrity of the Gram-negative bacterial cell surface by covalent

385   interaction between the C-terminal lysine and the *meso*-diaminopimelic acid residue of the PG layer

386   (Braun & Wolff, 1970; Hirota, Suzuki, Nishimura, & Yasuda, 1977; H. Suzuki et al., 1978; Zhang

387   & Wu, 1992; Zhang, Inouye, & Wu, 1992). Published data suggest that *lpp* deletion leads to rescue

388   of growth after inhibition of LspA and LolCDE (McLeod et al., 2015; Nickerson et al., 2018; Xiao

389   et al., 2012; Yakushi, Tajima, Matsuyama, & Tokuda, 1997a; Zwiebel et al., 1981) as well as rescue

390   of the temperature-sensitive *Salmonella typhimurium lgt* and *lnt* mutants (Gan, Gupta, Sankaran,

391   Schmid, & Wu, 1993; Gupta, Gan, Schmid, & Wu, 1993). While *E. coli lnt* is essential in the

392   absence of *lpp* (Robichon et al., 2005), Lpp overexpression in the *E. coli lnt* mutant leads to

393   bacterial cell growth arrest (Narita & Tokuda, 2011). Following up on data from Pailler et al., who

394   demonstrated that *lgt* is essential in BW25113, a derivative of *E. coli* K-12 strain BD792, and that

395   Lgt depletion leads to increased DNA leakage from the cell pole (Pailler et al., 2012), we

396   demonstrate that Lgt depletion in the clinical *E. coli* strain CFT073 leads to significant perturbations

397   to the bacterial cell envelope leading to increased sensitivity to antibiotics (Table 1), increased

398   serum killing (Figure 2d) and attenuated virulence *in vivo* (Figure 2g).

399   Based on this information and published reports, we had expected that deletion of *lpp* would

400   also lead to rescue of growth after depletion or pharmacologic inhibition of Lgt, but our data

401   demonstrate Lpp is in fact protective in cells treated with Lgti (Figure 5) or after Lgt depletion in

402   the CFT074Δ*lgt* inducible deletion strain (Figure 2h). Both Lgt depletion and inhibition leads to the

23

403   loss of PG tethering to the OM mediated by Lpp and Pal (Figure 5). Data demonstrating that cells

404   expressing the Lpp^{C21A} mutant contain significantly less PG-linked Lpp further supports our

405   conclusions that Lpp linkage to PG is negatively affected by Lgti. Although alternative hypotheses

406   remain to be tested, our findings suggest that efficient crosslinking of Lpp to PG occurs only after

407   diacylglyceryl modification of lipoprotein substrates by Lgt. Given that Lpp is critical for cell

408   envelope stiffness (Mathelié-Guinlet, Asmar, Collet, & Dufrêne, 2020), we propose that in the

409   absence of significant accumulation of DGPLP or other PG-linked Lpp forms, Lpp is protective

410   against Lgti bactericidal activity. While our data is consistent with a previous report demonstrating

411   UPLP and DGPLP are both linked to a single muropeptide unit (M. Suzuki et al., 2002), we show

412   that the level of PG-linkage is significantly less efficient in the absence of diacylglyceryl

413   modification of pro-Lpp. The consequence of these findings is that targeting Lgt as a novel

414   antibacterial target would overcome a major liability of targeting other steps in the lipoprotein

415   biosynthetic pathway, namely the off-target resistance mediated by *lpp* deletion (McLeod et al.,

416   2015; Xiao et al., 2012; Zwiebel et al., 1981).

417   The Lgti identified in this study are the first described inhibitors of the first committed step

418   in bacterial lipoprotein biosynthesis. G2823 and G2824 inhibit growth of WT *E. coli* and *A.*

419   *baumannii*. We used a combination of biochemical and genetic strategies (Figure 3) to confirm

420   these molecules function through inhibition of the diacylglyceryl transferase activity of Lgt. First,

421   the Lgti in this study were identified using a Lgt binding screen and confirmed to inhibit Lgt

422   enzymatic function *in vitro*. Second, the multiple effects and phenotypes detected in Lgti-treated

423   cells were recapitulated using *lgt* inducible deletion strains, strongly arguing against off-target

424   effects as the main cause of cell death. While we were unable to raise on-target resistant mutants to

425   any Lgti, one could speculate that if the Lgti bind to the conserved phosphatidylglycerol binding

426 site in Lgt, mutations disrupting Lgti binding might result in loss of Lgt function leading to cell

427 death. This hypothesis is actually consistent with data using globomycin or an improved analog

428 ,G0790, which binds a highly conserved active site (Vogeley et al., 2016) and for which no on-

429 target resistance mutations have ever been described (Lehman & Grabowicz, 2019; Pantua et al.,

430 2020). As recent publications have revealed significant insights into the potential mechanisms of

431 diacylglyceryl modification by Lgt (Mao et al., 2016; Singh et al., 2019), further studies aimed at

432 determining if these Lgti competitively inhibit binding of the phosphatidylglycerol or prolipoprotein

433 substrates would be critical in better understanding the mechanism by which these molecules

434 interfere with this critical OM biogenesis pathway. Although we do not detect MIC shifts with Lgti

435 in cells overexpressing *lgt* (data not shown), drug resistance in *E. coli* after target overexpression

436 can increase, remain unchanged or decrease depending on the balance between bacterial fitness

437 costs and inhibition of enzymatic activity (Palmer & Kishony, 2014). One could speculate that even

438 a modest inhibition of Lgt could lead to significant effects on OM integrity and cellular fitness

439 which may counteract any resistance arising from *lgt* overexpression. While CRISPRi-mediated

440 downregulation of *lgt* expression specifically sensitizes cells to Lgti but not LspAi or LolCDEi

441 (Figure 4g), *lolC* downregulation increases sensitivity to growth inhibition by LolCDE, Lgti and, at

442 higher concentrations, LspAi (Figure 4-supplement 1). It is possible that LolC depletion may

443 increase the permeability of cells to Lgti and LspAi as Lol depletion by CRISPRi has been

444 demonstrated to lead to increased risk of plasmolysis and membrane reorganization (Caro, Place, &

445 Mekalanos, 2019). As with many early antibiotic leads, we cannot fully rule out that the Lgti

446 identified in this study may have additional targets in bacterial cells at higher concentrations, but

447 our data strongly suggest that Lgti concentrations that inhibit growth of OM-permeabilized *E. coli*

448 are consistent with their inhibition of Lgt enzymatic activity.

449   In addition to the fact that *lpp* deletion does not play a role in resistance to Lgti, our studies

450   have uncovered additional novel findings that spur new questions and investigations. First, both

451   Lgt depletion as well as pharmacologic inhibition of Lgt led to accumulation of a ~14 kDa Lpp

452   isoform in the IM (Δ, Figure 5f,g). While the identity or function of this Lpp form is unknown, its

453   size and the fact that a Lpp form around the same molecular weight is also detected in cells

454   expressing the LppΔK mutant (Figure 5 – figure supplement 1) suggest that it could represent a

455   stable Lpp dimer. While stable Lpp trimers have been described (Bjelić, Karshikoff, & Jelesarov,

456   2006; Shu, Liu, Ji, & Lu, 2000), there is also evidence that Lpp can exist as a dimer (Chang, Lin,

457   Wang, & Liao, 2012). Second, while our data suggest that the lack of diacylglyceryl modification

458   by Lgt generates a less optimal substrate for the L,D-transpeptidases that covalently link Lpp to PG,

459   it does not rule out the possibility that PG-linkage may occur at or after modification by Lgt. Third,

460   we demonstrate that LolCDEi remain bactericidal against cells expressing only LppΔK. While the

461   sucrose gradient and sarkosyl solubilization centrifugation studies demonstrate that LspAi treatment

462   leads to accumulation of DGPLP in the IM (Figure 6), consistent with previous data with

463   globomycin (M. Suzuki et al., 2002), no such accumulation is detected after treatment with

464   LolCDEi. This raises the possibility that accumulation of either WT Lpp or LppΔK could compete

465   with less abundant essential OM lipoproteins for limited transport via LolCDE, which is consistent

466   with our data demonstrating decreased OM localization of BamD after LolCDEi treatment (Figure 6

467   – figure supplement 1). Lgti, like LspAi and LolCDEi, had significant effects on OM localization

468   of the β-barrel protein, OmpA (Figure 6a), which is most likely due to decreased OM expression of

469   BamD and consequently BamA (Figure 6 – figure supplement 1). These results inform us that

470   while Lgti behave very similarly to LspAi and LolCDEi in terms of depleting OM lipoproteins and

471   OMPs, their effects on Lpp set them apart from other inhibitors on this pathway.

26

472   In summary, our study is the first to systematically differentiate the role of Lpp in targeting

473   multiple steps of bacterial lipoprotein biosynthesis and transport. The loss of PG-association of Lpp

474   and Pal, resulting from Lgt depletion or pharmacologic inhibition of Lgt, leads to significant OM

475   defects. The identification and characterization of these Lgti validates Lgt as a novel and druggable

476   antibacterial target and could serve as initial starting points for ongoing medicinal chemistry efforts

477   to improve antibacterial potency and physiochemical properties. Our studies suggest that

478   therapeutic targeting of Lgt over other steps in the lipoprotein biosynthesis and transport pathways

479   might present a more favorable resistance profile and prevent the spread of multi-drug resistant

480   bacterial infections.

481

482

483

484

485

486

487

488

489

490

491 **Materials and Methods**

492

493 **Ethics statement**

494 All mice used in this study were housed and maintained at Genentech in accordance with American

495 Association of Laboratory Animal Care guidelines. All experimental studies were conducted under

496 protocol 13-0979A were approved by the Institutional Animal Care and Use Committee of

497 Genentech Lab Animal Research and performed in an Association for Assessment and

498 Accreditation of Laboratory Animal Care International (AAALAC)-accredited facility in

499 accordance with the Guide for the Care and Use of Laboratory Animals and applicable laws and

500 regulations.

501

502 **Antibodies**

503 The anti-Pal antibody was a generous gift from Dr. Shaw Warren (Massachusetts General Hospital).

504 The anti-OmpA (Antibody Research Corporation), anti-GroEL (Enzo Life Sciences), anti-ThyA

505 (GeneTex, Inc) and anti-His (Cell Signaling Technology) antibodies were obtained from

506 commercial sources. Generation of anti-Lpp and anti-BamA antibodies has been previously

507 described (Diao et al., 2017; Storek et al., 2018; 2019). Recombinant Lgt and BamD were used to

508 generate rabbit polyclonal antibodies. Rabbit immunizations, generation of antisera and purification

509 of rabbit polyclonal antibodies were performed as previously described for Lpp (Diao et al., 2017).

510

511 **Generation of bacterial strains and plasmids**

512   Bacterial strains and plasmids used in this study are listed in Supplemental File 2. *E. coli* strain

513   CFT073 (ATCC 700928) (Mobley et al., 1990) and MG1655 (ATCC 700926) were purchased from

514   ATCC. Gene disruption in CFT073 was performed as previously described (Datsenko & Wanner,

515   2000; Diao et al., 2017). CFT073Δ*lgt* was generated based on the previously published protocol

516   (Pailler et al., 2012) by retaining the *lgt* stop codon, which forms part of the *thyA* ribosomal binding

517   site. The primers used to generate the CFT073 and MG1655 mutants are listed in Supplemental

518   File 3. Plasmids pKD46 for the λ Red recombinase (Datsenko & Wanner, 2000; Diao et al., 2017),

519   pKD4 or pSim18 for the integration construction (Datsenko & Wanner, 2000; Diao et al., 2017) and

520   pCP20 (Cherepanov & Wackernagel, 1995) for the FLP recombinase were used in this study. The

521   inducible deletion strains (MG1655Δ*lgt*, MG1655Δ*lspA* and MG1655Δ*lolCDE*) in either the WT

522   and/or Δ*lpp* backgrounds were generated using similar methods as previously described (Diao et al.,

523   2017; Noland et al., 2017). CFT073*imp*4213Δ*lpp* containing pBAD24-*lpp* was used to generate

524   CFT073*imp*4213Δ*lpp:lpp*^{Ara} to detect the different Lpp species after treatment with pharmacologic

525   inhibitors. The PA14*imp*4213 strain was generated based on published protocols (Balibar &

526   Grabowicz, 2016; Hmelo et al., 2015). For expression under the IPTG-inducible promoter, DNA

527   encoding the full-length sequences of *lgt*, *lspA*, *lnt* and *lolCDE* were cloned into pLMG18 and

528   induced using 2.5 mM IPTG.

529

530   ***In vitro* growth inhibition and serum sensitivity assays**

531   Unless stated otherwise, *E. coli* cells were grown in Luria-Bertani (LB) medium (0.5% yeast

532   extract, 1% tryptone, 0.5% NaCl) at 37°C. When indicated, kanamycin (Kan) was added to culture

533   media at a 50 μg/ml final concentration. MIC assays were performed based on Clinical and

29

534   Laboratory Standards Institute (CLSI) guidelines. For *in vitro* growth curves, overnight cultures of

535   WT CFT073, CFT073Δ*lgt* and CFT073Δ*lgt* complemented with *lgt* from *E. coli* (*lgt* [Ec]) or *P.*

536   *aeruginosa* (*lgt* [Pa]) were grown to mid-exponential phase (OD_{600}=0.6) and then diluted to

537   OD_{600}=0.1 to initiate growth curves. At various times, culture aliquots were diluted and plated in

538   dilutions on LB+Kan agar and CFUs were enumerated in duplicate. Growth of MG1655 inducible

539   deletion strains was measured by culturing in the presence of two-fold dilutions of arabinose

540   (starting arabinose concentrations for CFT073 and MG1655 inducible deletion strains were 4% and

541   0.8%, respectively). While 2% arabinose was sufficient for WT growth of MG1655Δ*lgt,* 4%

542   arabinose was used for CFT073Δ*lgt* based on comparing its growth to that of WT CFT073 as

543   measured by CFUs. OD_{600} growth measurements were performed using an EnVision 2101

544   Multilabel Reader plate reader (PerkinElmer) linked with Echo Liquid Handler (Labcyte). For

545   time-kill experiments, bacteria were harvested in mid-exponential phase and treated with 12.5 μM

546   Lgti G2824, 3.2 μM LspAi (GBM), 6.3 μM LolCDEi (C1) and 1.6 μM vancomycin. G2823 was

547   not be tested due to limitations in compound availability. CFUs were enumerated at various times

548   post treatment. Bacterial culture medium containing 2% arabinose was used to induce *lpp* or *lpp*ΔK

549   expression from pBad24 plasmids. Bacterial viability at different time points during the treatment

550   was measured by enumerating CFU. Serum killing assays were carried out as previously described

551   (Diao et al., 2017).

552

553   **Detection of membrane permeability using SYTOX Green incorporation**

Inhibition of Lgt in Gram-negative bacteria

554   To determine the effect of Lgt depletion on membrane permeability, WT CFT073 and CFT073Δ*lgt*

555   strains were streaked onto a LB agar plate containing 4% arabinose and cultured at 37°C for 18

556   hours. From a single colony, bacteria were cultured in LB broth containing 4% arabinose and

557   cultured at 37°C to OD 0.5. One mL cultures of OD=0.5 for both strains were harvested, washed

558   and resuspended in LB broth or medium containing a range of arabinose (2, 0.2, 0.1, 0.05% and 0)

559   or glucose (0.2%) concentrations and incubated at 37°C for 2 hours. Cells were harvested by

560   centrifugation at $4000 \times g$ at 4°C for 5 minutes. Intact CFT073 or CFT073 treated with 70%

561   ethanol at RT for 15 minutes to permeabilize the cells were used as controls. Cells were incubated

562   with SYTOX green following the manufacturer's recommendation, washed with PBS (3×) and

563   fixed in 2% paraformaldehyde. SYTOX Green incorporation was measured by flow cytometry

564   using a FACS Aria II (Becton Dickenson) and analyzed using Flowjo software.

565

566   **Mouse infection model**

567   Overnight bacterial cultures were back diluted 1:100 in M9 media and grown to an OD_{600}=0.8-1 at

568   37°C. Cells were harvested, washed once with PBS and resuspended in PBS containing 10%

569   glycerol. Cells were frozen in aliquots and thawed aliquots were measured for CFUs prior to mouse

570   infections. Virulence of WT CFT073 and CFT073Δ*lgt* was measured using the neutropenic *E. coli*

571   infection model (Cross, Siegel, Byrne, Trautmann, & Finbloom, 1989). Seven-week-old female A/J

572   mice (Jackson Laboratory) were rendered neutropenic by peritoneal injection of 2 doses of

573   cyclophosphamide (150 mg/kg on Day -4 and 100 mg/kg on Day -1). On Day 0, mice were

574   infected with 5×10^5 CFU of mid-exponential phase bacteria diluted in PBS by intravenous

575   injection through the tail vein. At 30 minutes and 24 hours post infection, bacterial burden in the

576   liver and spleen was determined by serial dilutions of tissue homogenates on LB plates.

577

Macrocyclic peptide library design and selection of Lgt-binding molecules

579   A thioether-macrocyclic peptide library was constructed by using N-chroloacetyl D-phenylalanine

580   (ClAc-f) as an initiator in a genetically reprogrammed in vitro translation system (Kashiwagi et al.,

581   2013). The genetic code was designed with the addition of two N-methyl amino acids: N-methyl-L-

582   phenylalanine (MeF) and N-methyl-L-glycine (MeG); and, three unnatural amino acids: (S)-2-

583   aminoheptanoic acid (Ahp), (S)-3-([1,1'-biphenyl]-4-yl)-2-aminopropanoic acid (Bph), and (S)-

584   1,2,3,4-tetrahydroisoquinoline-3-carboxylic acid (Tic) in addition to 11 natural amino acids (Ser,

585   Tyr, Trp, Leu, Pro, His, Arg, Asn, Val, Asp, and Gly). After *in vitro* translation, a thioether bond

586   formed spontaneously between the N-terminal ClAc group of the initiator D-phenylalanine residue

587   and the sulfhydryl group of a downstream cysteine residue to generate the macrocyclic peptides.

588   Affinity selection of macrocyclic peptides binding to Lgt was performed using *E. coli* Lgt-

589   biotin in 0.02% n-dodecyl β-D-maltoside (DDM). Briefly, 10 μM mRNA library was hybridized

590   with a peptide-linker (11 μM) at RT for 3 minutes. The mRNA library was translated at 37°C for 30

591   minutes in the reprogrammed *in vitro* translation system to generate the peptide-mRNA fusion

592   library (Goto et al., 2011; Ishizawa et al., 2013). Each reaction contained 2 μM mRNA-peptide-

593   linker conjugate, 12.5 μM initiator tRNA (tRNAfMet aminoacylated with ClAc-D-Phe), and 25 μM

594   of each elongator tRNA aminoacylated with the specified non-canonical /canonical amino acids. In

595   the first round of selections, translation was performed at 20 μL scale. After the translation, the

596   reaction was quenched with 17 mM EDTA. The product was subsequently reverse-transcribed using

597   RNase H minus reverse transcriptase (Promega) at 42°C for 30 minutes and buffer was exchanged

598   for DDM buffer: 50 mM Tris (pH 8), 5 mM EDTA, 200 mM NaCl2, 0.02% DDM, and 1 mM

32

599 Glutathione. For affinity selection, the peptide-mRNA/cDNA solution was incubated with 250 nM

600 biotinylated *E. coli* Lgt for 60 minutes at 4°C and the streptavidin-coated beads (Dynabeads M-280

601 Streptavidin, Thermo) were further added and incubated for 10 minutes to isolate Lgt binders. The

602 beads were washed once with cold DDM buffer, the cDNA was eluted from the beads by heating

603 for 5 minutes at 95°C, and fractional recovery from the affinity selection step were assessed by

604 quantitative PCR using Sybr Green I on a LightCycler thermal cycler (Roche). After five rounds of

605 affinity maturation, two additional rounds of off-rate selections were performed by increasing the

606 wash stringency before elation to identify high affinity binders. Sequencing of the final enriched

607 cDNA was carried out using a MiSeq next generation sequencer (Illumina).

608

Peptide Synthesis

610 Thioether macrocyclic peptides were synthesized using standard Fmoc solid phase peptide synthesis

611 (SPPS). Following coupling of all amino acids, the deprotected N-terminus was chloroacetylated

612 on-resin followed by global deprotection using a trifluoroacetic acid (TFA) deprotection cocktail.

613 The peptides were then precipitated from the deprotection solution by adding over 10-fold excess

614 diethyl ether. Crude peptide pellets were then dissolved and re-pelleted 3 times using diethyl ether.

615 After the final wash, the pellet was left to dry and then the pellet was resuspended in DMSO

616 followed by the addition of triethylamine for intramolecular cyclization via formation of a thioether

617 bond between the thiol of the cysteine and N-terminal chloroacetyl group. Upon completion of

618 cyclization, the reaction was quenched with AcOH and the cyclic peptide was purified using

619 standard reverse-phase HPLC methods.

620

SDS-PAGE and Western immunoblotting

622 Bacterial cell samples normalized for equivalent OD_{600} and resuspended in Bugbuster lysis buffer

623 (Fischer Scientific) with the addition of sample buffer (LI-COR), and separated by SDS-PAGE

624 using 16% Tricine protein gels or NuPAGE 4-20% Bis-Tris gels (Thermofisher Scientific) and

625 transferred to nitrocellulose membranes using the iBlot™2 Dry Blotting system (Invitrogen) and

626 blocked using LI-COR blocking buffer for 30 minutes. Unless stated otherwise, loading buffer with

627 reducing agents were added and samples were not boiled prior to SDS-PAGE. For the sucrose

628 gradient centrifugation, samples were boiled prior to running the SDS-PAGE. Primary antibodies

629 were used at a final concentration of 1μg/ml with some exceptions: rabbit anti-Lpp polyclonal

630 antibody (0.1μg/ml); murine anti-Pal 6D7 (0.5 μg/ml); rabbit anti-GroEL (1:10,000 final dilution);

631 rabbit anti-OmpA (1:50,000 final dilution). The secondary antibodies were all obtained from LI-

632 COR, and used as per manufacturer's instructions. Images were collected using the Odyssey CLx

633 imaging system (LI-COR) and analyzed by Image Studio Lite.

634

635

Expression and purification of recombinant Lgt and BamD

637 DNA encoding full-length *E. coli* Lgt fused to a C-terminal Flag-tag was transformed into Rosetta

638 2(DE3) Gold cells (Agilent). Starter cultures were grown in Terrific Broth (TB) media with

639 carbenicillin (50μg/mL) and chloramphenicol (12.5μg/mL) at 37°C for 3 hours. The starter cultures

640 were diluted 1:50 in TB medium with carbenicillin (50μg/mL), chloramphenicol (12.5μg/mL), and

641 glycerol (1%) and grown at 37°C for 2 hours with shaking at 200 rpm. The temperature of the

642 culture was reduced to 30°C and grown for an additional 2 hours before the temperature of the

643 culture was reduced to 16°C and grown for 64 hours. The cells were harvested by centrifugation

644 and resuspended into lysis buffer (20mM Tris, pH 8.0, 300mM NaCl, Protease Inhibitor cocktail

645 and Lysonase) and stirred at 4°C for 30 minutes before being passed through a microfluidizer 3

646 times. The membrane fraction was solubilized by adding DDM directly to the lysate to a final

647 concentration of 1% and stirring at 4°C for 2 hours before centrifugation at 40,000 rpm for 1 hour.

648 Pre-equilibrated FLAG resin was added to the supernatant and incubated with rotation at 4°C for 2

649 hours. The slurry was added to a gravity column and the column was washed with 10 CV buffer A

650 (20mM Tris, pH 8.0, 300mM NaCl, 5% glycerol, 1% DDM) and 10 CV buffer B (20mM Tris, pH

651 8.0, 300mM NaCl, 5% glycerol, 0.05% DDM). The bound fraction was eluted by the addition of 5

652 CV of buffer C (20mM Tris, pH 8.0, 300mM NaCl, 5% glycerol, 0.05% DDM, 100μg/mL FLAG

653 peptide). The peak fractions were collected, concentrated to less than 5 mL and loaded onto a

654 superdex 200 16/60 column equilibrated with buffer C (20mM Tris, pH 8.0, 300mM NaCl, 5%

655 glycerol, 0.05% DDM, 1mM TCEP). The peak fractions were collected, analyzed by SDS-PAGE

656 and stored at -80°C.

657 For recombinant *E. coli* BamD protein expression, DNA fragments encoding BamD (Gly$_{22}$-

658 Thr$_{245}$) were cloned into a modified pET-52b expression vector containing an C-terminal His$_8$-tag

659 and overexpressed in *E. coli* host Rosetta 2 (DE3) grown by fermentation at 17°C for 64 hours, at

660 which point cells were collected and resuspended in 50 mM Tris, pH 8.0, 300 mM NaCl, 0.5 mM

661 TCEP containing cOmplete Protease Inhibitors (Roche), 1 mM PMSF and 2 U/ml of Benzonase

662 nuclease (Sigma Aldrich). After cell lysis by microfluidization and low speed centrifugation,

663 soluble protein was purified by Ni-NTA affinity and size exclusion chromatography. The peak

664 fractions containing BamD were pooled and concentrated to 5 mg/mL.

665

35

Development of the Lgt biochemical assay

666

667 The Lgt enzymatic activity was measured by specific detection of G3P. Both G3P and G1P are

668 released from phosphatidylglycerol as Lgt catalyzes the transfer of diacylglyceryl from

669 phosphatidylglycerol to the preprolipoprotein substrate, since the PG substrate used in the assay

670 contains a racemic glycerol moiety at the end of phosphatidyl group. The standard assay consists of

671 6 μL reaction mixture with 3 nM Lgt-DDM, 50 μM phosphatidylglycerol (1,2-dipalmitoyl-*sn*-

672 glycero-3-phospho-(1'-*rac*-glycerol), Avanti), 12.5 μM Pal-IAAC peptide substrate derived from

673 the Pal lipoprotein (MQLNKVLKGLMIALPVMAIAA<u>C</u>SSNKN, synthesized by CPC Scientific) in

674 50 mM Tris, pH 8, 200 mM NaCl, 5 mM EDTA, 0.02% DDM, 0.05 % Bovine Skin Gelatin, and 1

675 mM glutathione. As a control, we used a mutant non-modifiable Pal substrate peptide containing a

676 cysteine to alanine mutation (Pal-IAA**<u>A</u>**) which served as a competitive non-modifiable inhibitor.

677 The reaction was quenched after 60 minutes at RT with 0.5 μL of 4.8% Lauryl Dimethylamine-N-

678 Oxide (Anatrace), followed by addition of 6 μL Detection Solution. After incubation for 120

679 minutes at RT, the luminescence signal was read. The Detection Solution was modified based on a

680 NAD Glo protocol (Promega, G9072), per manufacturer's instruction. Specifically, 10 mL

681 Detection Solution consists of 3-fold dilution of Luciferin Detection Reagents, supplemented with

682 10 μL Reductase, 2.5 μL Reductase Substrate, 1 mM NAD, and 4.25 U of G3PDH (Roche

683 Diagnostics, 10127779001). The Luciferin Detection Reagents, Reductase, and Reductase Substrate

684 were all from the NAD Glo kit (Promega). Luminescence values were normalized to DMSO

685 controls (0% inhibition) and no enzyme controls (100% inhibition). IC_{50} values were calculated

686 using a 4 parameter logistic model using GraphPad Prism software.

687

688 Visualization of WT CFT073 and CFT073Δ*lgt* by time-lapse microcopy, confocal

36

689 **microcopy, transmission electron microscopy**

690 Electron microscopy was performed as previously described (Noland et al., 2017). For time-lapse

691 microscopy, WT CFT073, CFT073Δ*lgt* and CFT073Δ*lgt*Δ*lpp* cells were grown overnight in LB

692 medium containing 4% arabinose, back-diluted to a final OD_{600} of 0.1 and immediately placed

693 between a cover slip and 1% agarose pad containing 0.2% glucose for imaging. Cells were

694 maintained at 37 °C during imaging in a stage top chamber (Okolab Inc.). Cells were imaged on a

695 Nikon Eclipse Ti inverted confocal microscope (Nikon Instruments Inc.) coupled with a UltraVIEW

696 VoX (PerkinElmer Inc.) and a 100× (NA 1.40) oil-immersion objective. Images were captured at

697 various times using ORCA-Flash 4.0 CMOS camera (Hamamatsu Photonics), collected using

698 Volocity software (Quorum Technologies) and processed using Fiji (Schindelin et al., 2012). For

699 confocal microscopy, images were acquired on a Leica SP8 STED 3x platform using a 100× white

700 light, NA:1.4 oil immersion objective. CFT073*imp4213* cells were treated with Lgti, LspAi or

701 LolCDEi at 1×MIC for 30 minutes, fixed with 4% paraformaldehyde and incubated with 1 μg/mL

702 FM-64 dye and 1 μg/mL DAPI solution. Quantitation of bacterial cell area was performed using

703 the ImageJ program by measuring at least ~100 bacterial cells from two independent experiments.

704

705 **Targeted downregulation of gene expression by CRISPRi**

706 The two-plasmid bacterial CRISPRi system pdCas9-bacteria_GNE and pgRNA-bacteria_GNE are

707 based off the AddGene plasmids 44249 and 44251 (Qi et al., 2013), respectively. The plasmid was

708 synthesized in smaller DNA fragments (500bp-3kb) (IDT gBlocks) and assembled by Gibson

709 Assembly (NEB) according to manufacturer's protocols. Plasmids were confirmed by sequencing

710 (ELIM Bio). gRNAs were designed to target the 5' end of the gene on the non-template strand

711 using Benchling CRISPR software (Peters et al., 2016). gRNAs were cloned into pgRNA-bacteria

712   using Gibson Assembly (NEB) according to manufacturer's protocols and sequence confirmed

713   (ELIM Bio).

714   Bacterial cultures were grown overnight on LB agar supplemented with carbenicillin (50

715   μg/mL) and chloramphenicol (12.5 μg/mL) to maintain both plasmids, pdCas9-bacteria and

716   pgRNA-bacteria with each gRNA as appropriate. Cells were scraped from the plate into fresh

717   media. OD_{600} was measured and subsequently diluted to OD_{600}=0.001 in the presence or absence of

718   Lgti, LspAi and LolCDEi. 200 μL was transferred to a 96-well plate (Corning) and monitored for

719   growth by measuring OD_{600} (EnVision Multimode Plate Reader, PerkinElmer). All treatments were

720   performed in triplicate. Specificity of CRISPRi downregulation was measured using RT-qPCR.

721

722   **Purification of peptidoglycan-associated proteins**

723   Purification of PG-associated proteins (PAP) was performed according to published methods (Diao

724   et al., 2017; Nakae et al., 1979; Whitfield et al., 1983) with some modifications. Briefly, bacteria

725   were harvested in mid-exponential phase for treatment and then subjected for PAP extraction by

726   resuspended cell pellets from 10 OD (A_{600}) in 6 mL of PAP extraction buffer containing 2%

727   (wt/vol) SDS in 100 mM Tris-HCl (pH 8.0) with 100mM NaCl, 10% glycerol, and cOmplete^{TM},

728   mini, EDTA-free protease inhibitor cocktail (Sigma-Aldrich). After 60 minutes at RT, the

729   extraction was subjected to centrifugation at $100,000 \times g$ for 60 minutes at 22°C, and the pellet,

730   containing PG and associated proteins, was washed once with the same PAP extraction buffer with

731   centrifugation at $100,000 \times g$ for 30 minutes and resuspended in 200 μL of PAP extraction buffer

732   (referred to as the SDS-insoluble on PAP fraction). The supernatant containing the SDS-soluble

733   fraction was aliquoted and frozen (referred to as non-PAP fraction). Both fractions were treated

734   with equal volume of BugBuster buffer prior to the addition of sample buffer for Western

735   immunoblotting as described above. It should be noted that the final PAP fractions are ~30-fold

736   more concentrated than the non-PAP fractions.

737

738   **Isolation of *E. coli* IM and OM using sucrose gradient centrifugation and**

739   **sarkosyl fractionation**

740   Bacterial inner and outer membranes were separated by sucrose gradient as previously (Nickerson

741   et al., 2018; Yakushi, Tajima, Matsuyama, & Tokuda, 1997b) with some modifications. Briefly,

742   bacteria were grown in Luria broth at 37°C to mid-exponential phase (OD_{600}=0.6), and then treated

743   with 1×MIC of indicated inhibitors for 1 hour. Cells representing 30-40 OD_{600} equivalents were

744   harvested by centrifugation at 4000 × g for 15 minutes, washed once with 50 mM Tris-HCl (pH 7.5)

745   containing 25% (wt/vol) sucrose and Complete EDTA-free protease inhibitor cocktail (Roche), and

746   then incubated for 10 minutes at RT in the same buffer containing 100 μg/ml lysozyme (Thermo

747   Scientific) and 1000 U/ml nuclease (BenzonaseNuclease, EMD Millipore). Two-fold volume of

748   ice-cold EDTA (pH 8.0) was added and the suspension was disrupted by two passages through an

749   LV1 Microfluidizer (Microfluidics). Unbroken cells were removed by centrifugation at 4,000 × *g*

750   and membranes were collected by ultracentrifugation at 100,000 × *g* for 1 hour and washed once

751   with 50 mM Tris-HCl (pH 7.5). The final membrane preparation was resuspended in 50 mM Tris-

752   HCl (pH 7.5) containing 10% sucrose, 1.5 mM EDTA and protease inhibitor cocktail and then

753   applied to a 30 to 70% (wt/vol) sucrose gradient. The loaded gradients were spun at 200,000 × g for

754   22 hours at 4°C in a Beckman SW41Ti rotor. Fractions were removed and analyzed by SDS-PAGE

755   and immunoblotting with appropriate antibodies. The IM fractionation of bacterial cells using

756   sarkosyl was performed according to published methods (Filip et al., 1973; Pantua et al., 2020)..

757

758 **Statistical analyses**

759 All statistical analyses were performed using GraphPad Prism 6.0 software (GraphPad). The data

760 was tested for being parametric and statistical analyses were performed on log-transformed data.

761 All graphs represent the mean $\pm$ the standard error of the mean (SEM). Unless stated otherwise, p

762 values for all data were determined using regular unpaired *t* test (* = p<0.05, ** = p<0.01, and ***

763 = p<0.001). p values for mouse CFU studies were determined using the Mann Whitney Test.

764 Bonferroni correction was applied to control for multiple comparisons for CRIPSRi data in Figure

765 4g.

766

767 **Acknowledgements**

771

772 **Competing interests**

777

778

779

780 **References**

781 Balibar, C. J., & Grabowicz, M. (2016). Mutant Alleles of lptD Increase the Permeability of
782   Pseudomonas aeruginosa and Define Determinants of Intrinsic Resistance to Antibiotics.
783   *Antimicrobial Agents and Chemotherapy*, *60*(2), 845–854. http://doi.org/10.1128/AAC.01747-
784   15
785 Bjelić, S., Karshikoff, A., & Jelesarov, I. (2006). Stability and folding/unfolding kinetics of the
786   homotrimeric coiled coil Lpp-56. *Biochemistry*, *45*(29), 8931–8939.
787   http://doi.org/10.1021/bi0608156
788 Braun, V., & Wolff, H. (1970). The murein-lipoprotein linkage in the cell wall of Escherichia coli.
789   *European Journal of Biochemistry / FEBS*, *14*(2), 387–391.
790 Caro, F., Place, N. M., & Mekalanos, J. J. (2019). Analysis of lipoprotein transport depletion in
791   Vibrio cholerae using CRISPRi. *Proceedings of the National Academy of Sciences of the United
792   States of America*, *116*(34), 17013–17022. http://doi.org/10.1073/pnas.1906158116
793 Cascales, E., Bernadac, A., Gavioli, M., Lazzaroni, J.-C., & Lloubes, R. (2002). Pal lipoprotein of
794   Escherichia coli plays a major role in outer membrane integrity. *Journal of Bacteriology*,
795   *184*(3), 754–759.
796 Chang, T.-W., Lin, Y.-M., Wang, C.-F., & Liao, Y.-D. (2012). Outer membrane lipoprotein Lpp is
797   Gram-negative bacterial cell surface receptor for cationic antimicrobial peptides. *The Journal of
798   Biological Chemistry*, *287*(1), 418–428. http://doi.org/10.1074/jbc.M111.290361
799 Cherepanov, P. P., & Wackernagel, W. (1995). Gene disruption in Escherichia coli: TcR and KmR
800   cassettes with the option of Flp-catalyzed excision of the antibiotic-resistance determinant.
801   *Gene*, *158*(1), 9–14.
802 Clavel, T., Germon, P., Vianney, A., Portalier, R., & Lazzaroni, J. C. (1998). TolB protein of
803   Escherichia coli K-12 interacts with the outer membrane peptidoglycan-associated proteins Pal,
804   Lpp and OmpA. *Molecular Microbiology*, *29*(1), 359–367.
805 Cowles, C. E., Li, Y., Semmelhack, M. F., Cristea, I. M., & Silhavy, T. J. (2011). The free and
806   bound forms of Lpp occupy distinct subcellular locations in Escherichia coli. *Molecular
807   Microbiology*, *79*(5), 1168–1181. http://doi.org/10.1111/j.1365-2958.2011.07539.x
808 Cross, A. S., Siegel, G., Byrne, W. R., Trautmann, M., & Finbloom, D. S. (1989). Intravenous
809   immune globulin impairs anti-bacterial defences of a cyclophosphamide-treated host. *Clinical
810   and Experimental Immunology*, *76*(2), 159–164.
811 Datsenko, K. A., & Wanner, B. L. (2000). One-step inactivation of chromosomal genes in
812   Escherichia coli K-12 using PCR products. *Proceedings of the National Academy of Sciences of
813   the United States of America*, *97*(12), 6640–6645. http://doi.org/10.1073/pnas.120163297
814 Dev, I. K., Harvey, R. J., & Ray, P. H. (1985). Inhibition of prolipoprotein signal peptidase by
815   globomycin. *The Journal of Biological Chemistry*, *260*(10), 5891–5894.
816 Diao, J., Bouwman, C., Yan, D., Kang, J., Katakam, A. K., Liu, P., et al. (2017). Peptidoglycan
817   Association of Murein Lipoprotein Is Required for KpsD-Dependent Group 2 Capsular
818   Polysaccharide Expression and Serum Resistance in a Uropathogenic Escherichia coli Isolate.
819   *mBio*, *8*(3), e00603–17. http://doi.org/10.1128/mBio.00603-17
820 Ferrer-Navarro, M., Ballesté-Delpierre, C., Vila, J., & Fàbrega, A. (2016). Characterization of the
821   outer membrane subproteome of the virulent strain Salmonella Typhimurium SL1344. *Journal
822   of Proteomics*, *146*, 141–147. http://doi.org/10.1016/j.jprot.2016.06.032

823   Filip, C., Fletcher, G., Wulff, J. L., & Earhart, C. F. (1973). Solubilization of the cytoplasmic
824   membrane of Escherichia coli by the ionic detergent sodium-lauryl sarcosinate. *Journal of*
825   *Bacteriology*, *115*(3), 717–722.

826   Gan, K., Gupta, S. D., Sankaran, K., Schmid, M. B., & Wu, H. C. (1993). Isolation and
827   characterization of a temperature-sensitive mutant of Salmonella typhimurium defective in
828   prolipoprotein modification. *The Journal of Biological Chemistry*, *268*(22), 16544–16550.

829   Gan, K., Sankaran, K., Williams, M. G., Aldea, M., Rudd, K. E., Kushner, S. R., & Wu, H. C.
830   (1995). The umpA gene of Escherichia coli encodes phosphatidylglycerol:prolipoprotein
831   diacylglyceryl transferase (lgt) and regulates thymidylate synthase levels through translational
832   coupling. *Journal of Bacteriology*, *177*(7), 1879–1882.

833   Gerth, K., Irschik, H., Reichenbach, H., & Trowitzsch, W. (1982). The myxovirescins, a family of
834   antibiotics from Myxococcus virescens (Myxobacterales). *The Journal of Antibiotics*, *35*(11),
835   1454–1459.

836   Goto, Y., Katoh, T., & Suga, H. (2011). Flexizymes for genetic code reprogramming. *Nature*
837   *Protocols*, *6*(6), 779–790. http://doi.org/10.1038/nprot.2011.331

838   Gupta, S. D., Gan, K., Schmid, M. B., & Wu, H. C. (1993). Characterization of a temperature-
839   sensitive mutant of Salmonella typhimurium defective in apolipoprotein N-acyltransferase. *The*
840   *Journal of Biological Chemistry*, *268*(22), 16551–16556.

841   Hirota, Y., Suzuki, H., Nishimura, Y., & Yasuda, S. (1977). On the process of cellular division in
842   Escherichia coli: a mutant of E. coli lacking a murein-lipoprotein. *Proceedings of the National*
843   *Academy of Sciences of the United States of America*, *74*(4), 1417–1420.

844   Hmelo, L. R., Borlee, B. R., Almblad, H., Love, M. E., Randall, T. E., Tseng, B. S., et al. (2015).
845   Precision-engineering the Pseudomonas aeruginosa genome with two-step allelic exchange.
846   *Nature Protocols*, *10*(11), 1820–1841. http://doi.org/10.1038/nprot.2015.115

847   Hobb, R. I., Fields, J. A., Burns, C. M., & Thompson, S. A. (2009). Evaluation of procedures for
848   outer membrane isolation from Campylobacter jejuni. *Microbiology (Reading, England)*,
849   *155*(Pt 3), 979–988. http://doi.org/10.1099/mic.0.024539-0

850   Igarashi, M. (2019). New natural products to meet the antibiotic crisis: a personal journey. *The*
851   *Journal of Antibiotics*, *72*(12), 890–898. http://doi.org/10.1038/s41429-019-0224-6

852   Inukai, M., Enokita, R., Torikata, A., Nakahara, M., Iwado, S., & Arai, M. (1978a). Globomycin, a
853   new peptide antibiotic with spheroplast-forming activity. I. Taxonomy of producing organisms
854   and fermentation. *The Journal of Antibiotics*, *31*(5), 410–420.
855   http://doi.org/10.7164/antibiotics.31.410

856   Inukai, M., Nakajima, M., Osawa, M., Haneishi, T., & Arai, M. (1978b). Globomycin, a new
857   peptide antibiotic with spheroplast-forming activity. II. Isolation and physico-chemical and
858   biological characterization. *The Journal of Antibiotics*, *31*(5), 421–425.
859   http://doi.org/10.7164/antibiotics.31.421

860   Ishizawa, T., Kawakami, T., Reid, P. C., & Murakami, H. (2013). TRAP display: a high-speed
861   selection method for the generation of functional polypeptides. *Journal of the American*
862   *Chemical Society*, *135*(14), 5433–5440. http://doi.org/10.1021/ja312579u

863   Jabbour, R. E., Wade, M. M., Deshpande, S. V., Stanford, M. F., Wick, C. H., Zulich, A. W., &
864   Snyder, A. P. (2010). Identification of Yersinia pestis and Escherichia coli strains by whole cell
865   and outer membrane protein extracts with mass spectrometry-based proteomics. *Journal of*
866   *Proteome Research*, *9*(7), 3647–3655. http://doi.org/10.1021/pr100402y

867   Kashiwagi, K., Reid, C. P., & Inc, P. (2013). Rapid display method in translational synthesis of
868   peptide.

869   Kitamura, S., Owensby, A., Wall, D., & Wolan, D. W. (2018). Lipoprotein Signal Peptidase
870   Inhibitors with Antibiotic Properties Identified through Design of a Robust In Vitro HT
871   Platform. *Cell Chemical Biology*, *25*(3), 301–308.e12.
872   http://doi.org/10.1016/j.chembiol.2017.12.011
873   Kovacs-Simon, A., Titball, R. W., & Michell, S. L. (2011). Lipoproteins of bacterial pathogens.
874   *Infection and Immunity*, *79*(2), 548–561. http://doi.org/10.1128/IAI.00682-10
875   Kowata, H., Tochigi, S., Kusano, T., & Kojima, S. (2016). Quantitative measurement of the outer
876   membrane permeability in Escherichia coli lpp and tol-pal mutants defines the significance of
877   Tol-Pal function for maintaining drug resistance. *The Journal of Antibiotics*.
878   http://doi.org/10.1038/ja.2016.50
879   Leduc, M., Ishidate, K., Shakibai, N., & Rothfield, L. (1992). Interactions of Escherichia coli
880   membrane lipoproteins with the murein sacculus. *Journal of Bacteriology*, *174*(24), 7982–7988.
881   Lehman, K. M., & Grabowicz, M. (2019). Countering Gram-Negative Antibiotic Resistance:
882   Recent Progress in Disrupting the Outer Membrane with Novel Therapeutics. *Antibiotics
883   (Basel, Switzerland)*, *8*(4), 163. http://doi.org/10.3390/antibiotics8040163
884   Mao, G., Zhao, Y., Kang, X., Li, Z., Zhang, Y., Wang, X., et al. (2016). Crystal structure of E. coli
885   lipoprotein diacylglyceryl transferase. *Nature Communications*, *7*, 10198.
886   http://doi.org/10.1038/ncomms10198
887   Mathelié-Guinlet, M., Asmar, A. T., Collet, J.-F., & Dufrêne, Y. F. (2020). Lipoprotein Lpp
888   regulates the mechanical properties of the E. coli cell envelope. *Nature Communications*, *11*(1),
889   1789–11. http://doi.org/10.1038/s41467-020-15489-1
890   McLeod, S. M., Fleming, P. R., MacCormack, K., McLaughlin, R. E., Whiteaker, J. D., Narita, S.-
891   I., et al. (2015). Small molecule inhibitors of Gram-negative lipoprotein trafficking discovered
892   by phenotypic screening. *Journal of Bacteriology*, *197*(6), JB.02352–14–1082.
893   http://doi.org/10.1128/JB.02352-14
894   Mizuno, T. (1979). A novel peptidoglycan-associated lipoprotein found in the cell envelope of
895   Pseudomonas aeruginosa and Escherichia coli. *Journal of Biochemistry*, *86*(4), 991–1000.
896   Mobley, H. L., Green, D. M., Trifillis, A. L., Johnson, D. E., Chippendale, G. R., Lockatell, C. V.,
897   et al. (1990). Pyelonephritogenic Escherichia coli and killing of cultured human renal proximal
898   tubular epithelial cells: role of hemolysin in some strains. *Infection and Immunity*, *58*(5), 1281–
899   1289.
900   Nakae, T., Ishii, J., & Tokunaga, M. (1979). Subunit structure of functional porin oligomers that
901   form permeability channels in the other membrane of Escherichia coli. *The Journal of
902   Biological Chemistry*, *254*(5), 1457–1461.
903   Narita, S.-I. (2011). ABC transporters involved in the biogenesis of the outer membrane in gram-
904   negative bacteria. *Bioscience, Biotechnology, and Biochemistry*, *75*(6), 1044–1054.
905   http://doi.org/10.1271/bbb.110115
906   Narita, S.-I., & Tokuda, H. (2010). Sorting of bacterial lipoproteins to the outer membrane by the
907   Lol system. *Methods in Molecular Biology (Clifton, NJ)*, *619*(Chapter 7), 117–129.
908   http://doi.org/10.1007/978-1-60327-412-8_7
909   Narita, S.-I., & Tokuda, H. (2011). Overexpression of LolCDE allows deletion of the Escherichia
910   coli gene encoding apolipoprotein N-acyltransferase. *Journal of Bacteriology*, *193*(18), 4832–
911   4840. http://doi.org/10.1128/JB.05013-11
912   Neidhardt, F. C. (1996). Chemical composition of *Escherichia coli*. In *Escherichia coli and
913   Salmonella: cellular and molecular biology* (2nd ed., pp. 1035–1063). Washington D.C.

Inhibition of Lgt in Gram-negative bacteria

914 Nickerson, N. N., Jao, C. C., Xu, Y., Quinn, J., Skippington, E., Alexander, M. K., et al. (2018). A
915   Novel Inhibitor of the LolCDE ABC Transporter Essential for Lipoprotein Trafficking in
916   Gram-Negative Bacteria. *Antimicrobial Agents and Chemotherapy*, *62*(4), e02151–17.
917   http://doi.org/10.1128/AAC.02151-17
918 Noland, C. L., Kattke, M. D., Diao, J., Gloor, S. L., Pantua, H., Reichelt, M., et al. (2017).
919   Structural insights into lipoprotein N-acylation by Escherichia coli apolipoprotein N-
920   acyltransferase. *Proceedings of the National Academy of Sciences of the United States of
921   America*, *114*(30), E6044–E6053. http://doi.org/10.1073/pnas.1707813114
922 Olatunji, S., Yu, X., Bailey, J., Huang, C.-Y., Zapotoczna, M., Bowen, K., et al. (2020). Structures
923   of lipoprotein signal peptidase II from Staphylococcus aureus complexed with antibiotics
924   globomycin and myxovirescin. *Nature Communications*, *11*(1), 140–11.
925   http://doi.org/10.1038/s41467-019-13724-y
926 Pailler, J., Aucher, W., Pires, M., & Buddelmeijer, N. (2012). Phosphatidylglycerol::prolipoprotein
927   diacylglyceryl transferase (Lgt) of Escherichia coli has seven transmembrane segments, and its
928   essential residues are embedded in the membrane. *Journal of Bacteriology*, *194*(9), 2142–2151.
929   http://doi.org/10.1128/JB.06641-11
930 Palmer, A. C., & Kishony, R. (2014). Opposing effects of target overexpression reveal drug
931   mechanisms. *Nature Communications*, *5*, 4296. http://doi.org/10.1038/ncomms5296
932 Pantua, H., Skippington, E., braun, M.-G., Noland, C. L., Diao, J., peng, Y., et al. (2020). Unstable
933   Mechanisms of Resistance to Inhibitors of Escherichia coli Lipoprotein Signal Peptidase. *mBio*,
934   *11*(5), VMBF–0016–2015. http://doi.org/10.1128/mBio.02018-20
935 Peters, J. M., Colavin, A., Shi, H., Czarny, T. L., Larson, M. H., Wong, S., et al. (2016). A
936   Comprehensive, CRISPR-based Functional Analysis of Essential Genes in Bacteria. *Cell*,
937   *165*(6), 1493–1506. http://doi.org/10.1016/j.cell.2016.05.003
938 Qi, L. S., Larson, M. H., Gilbert, L. A., Doudna, J. A., Weissman, J. S., Arkin, A. P., & Lim, W. A.
939   (2013). Repurposing CRISPR as an RNA-guided platform for sequence-specific control of gene
940   expression. *Cell*, *152*(5), 1173–1183. http://doi.org/10.1016/j.cell.2013.02.022
941 Robichon, C., Vidal-Ingigliardi, D., & Pugsley, A. P. (2005). Depletion of apolipoprotein N-
942   acyltransferase causes mislocalization of outer membrane lipoproteins in Escherichia coli. *The
943   Journal of Biological Chemistry*, *280*(2), 974–983. http://doi.org/10.1074/jbc.M411059200
944 Rojas, E. R., Billings, G., Odermatt, P. D., Auer, G. K., Zhu, L., Miguel, A., et al. (2018). The outer
945   membrane is an essential load-bearing element in Gram-negative bacteria. *Nature*, *559*(7715),
946   617–621. http://doi.org/10.1038/s41586-018-0344-3
947 Rossiter, S. E., Fletcher, M. H., & Wuest, W. M. (2017). Natural Products as Platforms To
948   Overcome Antibiotic Resistance. *Chemical Reviews*, *117*(19), 12415–12474.
949   http://doi.org/10.1021/acs.chemrev.7b00283
950 Rousset, F., Cui, L., Siouve, E., Becavin, C., Depardieu, F., & Bikard, D. (2018). Genome-wide
951   CRISPR-dCas9 screens in E. coli identify essential genes and phage host factors. *PLoS
952   Genetics*, *14*(11), e1007749. http://doi.org/10.1371/journal.pgen.1007749
953 Ruiz, N., Falcone, B., Kahne, D., & Silhavy, T. J. (2005). Chemical conditionality: a genetic
954   strategy to probe organelle assembly. *Cell*, *121*(2), 307–317.
955   http://doi.org/10.1016/j.cell.2005.02.014
956 Sankaran, K., & Wu, H. C. (1994). Lipid modification of bacterial prolipoprotein. Transfer of
957   diacylglyceryl moiety from phosphatidylglycerol. *The Journal of Biological Chemistry*,
958   *269*(31), 19701–19706.

959 Schindelin, J., Arganda-Carreras, I., Frise, E., Kaynig, V., Longair, M., Pietzsch, T., et al. (2012).
960   Fiji: an open-source platform for biological-image analysis. *Nature Methods*, *9*(7), 676–682.
961   http://doi.org/10.1038/nmeth.2019
962 Schlesinger, M. J. (1992). Lipid Modifications of Proteins. CRC Press.
963 Shu, W., Liu, J., Ji, H., & Lu, M. (2000). Core structure of the outer membrane lipoprotein from
964   Escherichia coli at 1.9 A resolution. *Journal of Molecular Biology*, *299*(4), 1101–1112.
965   http://doi.org/10.1006/jmbi.2000.3776
966 Silhavy, T. J., Kahne, D., & Walker, S. (2010). The bacterial cell envelope. *Cold Spring Harbor*
967   *Perspectives in Biology*, *2*(5), a000414–a000414. http://doi.org/10.1101/cshperspect.a000414
968 Singh, W., Bilal, M., McClory, J., Dourado, D., Quinn, D., Moody, T. S., et al. (2019). Mechanism
969   of Phosphatidylglycerol Activation Catalyzed by Prolipoprotein Diacylglyceryl Transferase.
970   *The Journal of Physical Chemistry. B*, *123*(33), 7092–7102.
971   http://doi.org/10.1021/acs.jpcb.9b04227
972 Stoll, H., Dengjel, J., Nerz, C., & Götz, F. (2005). Staphylococcus aureus deficient in lipidation of
973   prelipoproteins is attenuated in growth and immune activation. *Infection and Immunity*, *73*(4),
974   2411–2423. http://doi.org/10.1128/IAI.73.4.2411-2423.2005
975 Storek, K. M., Auerbach, M. R., Shi, H., Garcia, N. K., Sun, D., Nickerson, N. N., et al. (2018).
976   Monoclonal antibody targeting the β-barrel assembly machine of Escherichia coli is
977   bactericidal. *Proceedings of the National Academy of Sciences of the United States of America*,
978   *115*(14), 3692–3697. http://doi.org/10.1073/pnas.1800043115
979 Storek, K. M., Chan, J., Vij, R., Chiang, N., Lin, Z., Bevers, J., et al. (2019). Massive antibody
980   discovery used to probe structure-function relationships of the essential outer membrane protein
981   LptD. *eLife*, *8*, 3002. http://doi.org/10.7554/eLife.46258
982 Suzuki, H., Nishimura, Y., Yasuda, S., Nishimura, A., Yamada, M., & Hirota, Y. (1978). Murein-
983   lipoprotein of Escherichia coli: a protein involved in the stabilization of bacterial cell envelope.
984   *Molecular & General Genetics : MGG*, *167*(1), 1–9.
985 Suzuki, M., Hara, H., & Matsumoto, K. (2002). Envelope disorder of Escherichia coli cells lacking
986   phosphatidylglycerol. *Journal of Bacteriology*, *184*(19), 5418–5425.
987   http://doi.org/10.1128/jb.184.19.5418-5425.2002
988 Tokunaga, M., Tokunaga, H., & Wu, H. C. (1982). Post-translational modification and processing
989   of Escherichia coli prolipoprotein in vitro. *Proceedings of the National Academy of Sciences of*
990   *the United States of America*, *79*(7), 2255–2259. http://doi.org/10.1073/pnas.79.7.2255
991 Vogeley, L., Arnaout, El, T., Bailey, J., Stansfeld, P. J., Boland, C., & Caffrey, M. (2016).
992   Structural basis of lipoprotein signal peptidase II action and inhibition by the antibiotic
993   globomycin. *Science (New York, N.Y.)*, *351*(6275), 876–880.
994   http://doi.org/10.1126/science.aad3747
995 Whitfield, C., Hancock, R. E., & Costerton, J. W. (1983). Outer membrane protein K of Escherichia
996   coli: purification and pore-forming properties in lipid bilayer membranes. *Journal of*
997   *Bacteriology*, *156*(2), 873–879.
998 Wilson, M. M., & Bernstein, H. D. (2015). Surface-Exposed Lipoproteins: An Emerging Secretion
999   Phenomenon in Gram-Negative Bacteria. *Trends in Microbiology*.
1000   http://doi.org/10.1016/j.tim.2015.11.006
1001 Xiao, Y., Gerth, K., Müller, R., & Wall, D. (2012). Myxobacterium-produced antibiotic TA
1002   (myxovirescin) inhibits type II signal peptidase. *Antimicrobial Agents and Chemotherapy*,
1003   *56*(4), 2014–2021. http://doi.org/10.1128/AAC.06148-11

1004   Yakushi, T., Tajima, T., Matsuyama, S., & Tokuda, H. (1997a). Lethality of the covalent linkage
1005   between mislocalized major outer membrane lipoprotein and the peptidoglycan of Escherichia
1006   coli. *Journal of Bacteriology*, *179*(9), 2857–2862.
1007   Yakushi, T., Tajima, T., Matsuyama, S., & Tokuda, H. (1997b). Lethality of the covalent linkage
1008   between mislocalized major outer membrane lipoprotein and the peptidoglycan of Escherichia
1009   coli. *Journal of Bacteriology*, *179*(9), 2857–2862.
1010   Yem, D. W., & Wu, H. C. (1978). Physiological characterization of an Escherichia coli mutant
1011   altered in the structure of murein lipoprotein. *Journal of Bacteriology*, *133*(3), 1419–1426.
1012   Zhang, W. Y., & Wu, H. C. (1992). Alterations of the carboxyl-terminal amino acid residues of
1013   Escherichia coli lipoprotein affect the formation of murein-bound lipoprotein. *The Journal of
1014   Biological Chemistry*, *267*(27), 19560–19564.
1015   Zhang, W. Y., Inouye, M., & Wu, H. C. (1992). Neither lipid modification nor processing of
1016   prolipoprotein is essential for the formation of murein-bound lipoprotein in Escherichia coli.
1017   *The Journal of Biological Chemistry*, *267*(27), 19631–19635.
1018   Zwiebel, L. J., Inukai, M., Nakamura, K., & Inouye, M. (1981). Preferential selection of deletion
1019   mutations of the outer membrane lipoprotein gene of Escherichia coli by globomycin. *Journal
1020   of Bacteriology*, *145*(1), 654–656.

1021

1022

1023

1024

1025

1026

1027

1028

1029

1030

1031

1032

1033

1034 **Figure legends**

1035

1036 **Figure 1: Lipoprotein biosynthesis and transport in Gram-negative bacteria.** Prolipoprotein

1037 substrates translocate through the IM via the Sec or Tat pathway and are sequentially modified by

1038 Lgt, LspA and Lnt. Triacylated lipoproteins that are destined for the OM are recognized by the Lol

1039 system (LolABCDE) and transported to the OM. Lpp and Pal are two OM lipoproteins that tether

1040 the OM to the PG layer. Pal also binds to TolB, which also can interact with Lpp and OmpA, an

1041 OM β-barrel protein that can also associate with PG (not shown).

1042

1043 **Figure 2: Lgt is essential for *in vitro* growth, membrane integrity, serum resistance and**

1044 **virulence. (a)** CFT073Δ*lgt* cells were grown in the presence of 4% arabinose (red circles) or 0.2%

1045 glucose (grey circles) and CFUs were enumerated over 7 hours post treatment. CFT073Δ*lgt*

1046 cultured in the presence of 0.2% glucose were complemented with empty pLMG18 plasmid (open

1047 green triangles) or pLMG18 plasmids expressing *lgt* from *E. coli* (blue circles), *A. baumannii*

1048 (magenta circles) or *P. aeruginosa* (orange circles). The grey dashed line represents the limit of

1049 detection (200 CFU/ml) of the experiment. Data are representative of two independent experiments

1050 each performed in duplicate. **(b-c)** A modest ~25% reduction in Lgt levels results in a significant

1051 loss in viability over time with a concurrent accumulation of the unmodified pro-Lpp (ø, UPLP).

1052 CFT073Δ*lgt* cells were treated with a range of arabinose concentrations and CFUs were enumerated

1053 over 20 hours. CFU growth data are representative of two independent experiments each performed

1054 in duplicate. Western blot analysis for expression of Lgt and Lpp was performed using WT

1055   CFT073 and CFT073Δ*lgt* total cell lysates harvested at 3 hours post arabinose treatment. To

1056   quantitate Lgt expression levels, Lgt levels were normalized to GroEL and quantitated as fold

1057   change relative to WT CFT073 (FC vs WT). Lpp forms are denoted as follows: * = triacylated free

1058   Lpp; § = PG-linked diacylglyceryl pro-Lpp (DGPLP); ø = unmodified pro-Lpp (UPLP). Data are

1059   representative of two independent experiments. **(d)** Lgt depletion leads to increased serum

1060   sensitivity. WT CFT073 and CFT073Δ*lgt* cells grown in the presence of a range of arabinose

1061   concentrations (2% = magenta; 0.2% = light blue; 0.1% = green and 0.05% = orange) were

1062   incubated with 50% normal human serum (nHS), heat inactivated human serum (HIHS) or medium

1063   (no serum) for 1 hour and CFUs were enumerated. Data are representative of at least three

1064   independent experiments each performed in duplicate. **(e)** Lgt depletion leads to increased OM

1065   permeability. WT CFT073 and CFT073Δ*lgt* cells were incubated with the same range of arabinose

1066   concentrations as in Figure 2d and incubated with the nucleic acid dye, SYTOX Green, and flow

1067   cytometry was performed to determine level of dye incorporation. While SYTOX Green does not

1068   efficiently incorporate in bacterial cells with an intact OM (CFT073Δ*lgt* treated with 2% arabinose,

1069   magenta), SYTOX Green incorporation in bacterial cells increases after Lgt depletion. Intact

1070   CFT073 (WT, grey) or CFT073 treated with 70% ethanol (WT+ETOH, black), which permeabilizes

1071   the cells, were used as controls. Data are representative of two independent experiments. **(f)** Lgt

1072   depletion results in a globular cellular phenotype and membrane blebbing. WT CFT073 or

1073   CFT073Δ*lgt* cells were grown in either arabinose or glucose for 4 hours, fixed and incubated with

1074   FM-64 dye (red) and DAPI (blue) to detect OM and nucleic acids, respectively. Cells were

1075   visualized by confocal microscopy. Arrows represent membrane blebs. Scale bars represent 1 μm.

1076   Quantitation of cell size was performed using ImageJ software. **(g)** Lgt depletion leads to

1077   significant attenuation in virulence. Intravenous infection of neutropenic A/J mice with WT

1078   CFT073 (black) or CFT073Δ*lgt* (red) cells. At 0.5 hours and 24 hours post-infection, bacterial

1079   burden in the liver and spleen were enumerated. Overall *p*-value for the ANOVA is *p* <0.0001.

1080   Pairwise comparisons were analyzed using unpaired Mann Whitney test (** *p* = 0.0079). The grey

1081   dashed line represents the limit of detection (200 CFU/ml) for this experiment. **(h)** Deletion of *lpp*

1082   does not rescue growth after Lgt depletion. *E. coli* MG1655 (WT, black), or inducible deletion

1083   strains for *lgt* (Δ*lgt*, red), *lspA* (Δ*lspA, green)* and *lolCDE* (Δ*lolCDE*, blue) that either contained *lpp*

1084   or had *lpp* deleted were grown in conditions that allowed for normal growth (Ara^{WT}, 2% arabinose)

1085   or decreased growth (Ara^{Low}, 0.0125% arabinose) and CFUs at were enumerated at 5 hours post

1086   treatment. Data are representative of two independent experiments each performed in duplicate (*ns*

1087   = not significant, *p < 0.05, **p < 0.01).

1088

1089   **Figure 3: Identification of Lgt inhibitors. (a)** Representation of macrocycle peptide libraries

1090   varying in size from 8-14 amino acids in length. The variable region (X_n) of the macrocycle

1091   libraries was encoded to allow the random incorporation of 11 natural amino acids and 5 non-

1092   natural amino acids. **(b)** The 5 non-natural amino acids used in the generation of the libraries were

1093   N-α-Methyl-L-phenylalanine (MeF), N-α-Methyl-L-glycine (MeG, Sarcosine), (S)-2-

1094   Aminoheptanoic acid (Ahp), 4-Phenyl-L-phenylalanine (Bph) and (S)-1,2,3,4-

1095   Tetrahydroisoquinoline-3-carboxylic acid (Tic). **(c)** Schematic representation of affinity-based

1096   selections using recombinant Lgt-biotin immobilized on streptavidin magnetic beads. As discussed

1097   in the Methods, Lgt-DDM was incubated with the macrocycle library and Lgt binders were eluted,

1098   amplified and translated to generate new libraries enriched for Lgt binders. Iterative rounds of

1099   affinity selection and washing were performed against recombinant Lgt and macrocycles that bound

1100   to Lgt were identified using next generation sequencing. **(d)** Structure of the macrocyclic peptides

1101   G9066, G2823 and G2824 identified in this study. **(e)** Development of the *in vitro* Lgt biochemical

1102   assay. Lgt-DDM was incubated with phosphatidylglycerol and the Pal-IAAC peptide substrate

1103   derived from the Pal lipoprotein (MQLNKVLKGLMIALPVMAIAA<u>C</u>SSNKN) for 60 minutes at

1104   RT, as described in the Methods. After Lgt catalyzes the transfer of diacylglyceryl from

1105   phosphatidylglycerol to the Pal substrate (Pal-IAAC), glycerol-1-phosphophate (G1P) is released

1106   from phosphatidylglycerol. Given the phosphatidylglycerol substrate used in our biochemical assay

1107   contains a racemic glycerol moiety at the end of phosphatidyl group, both G1P and G3P are

1108   released. G3P is quantitatively converted to Dihydroxyacetone phosphate (DHAP) with

1109   concomitant formation of an equivalent amount of NADH by the action of glycerol 3-phosphate

1110   dehydrogenase (G3PDH). Newly formed NADH will in turn quantitatively react with

1111   proluciferin to generate equivalent amounts of luciferin, which ultimately results in

1112   luminescence by luciferase that is proportional to the amount of luciferin available. **(f)** Dose-

1113   dependent inhibition of Lgt biochemical activity. Lgt was incubated with phosphatidylglycerol and

1114   the Pal-IAAC substrate in the presence of absence of by G9066 (red), G2823 (green) or G2824

1115   (blue). Luminescence values were normalized to DMSO controls (0% inhibition) and no enzyme

1116   controls (100% inhibition). As a control, we incubated the Lgt reactions with a mutant substrate

1117   peptide also derived from the Pal lipoprotein which has the conserved cysteine mutated to alanine

1118   (Pal-IAA<u>**A**</u>, black). While the Pal-IAA<u>**A**</u> peptide binds to Lgt, it cannot be modified by Lgt and acts

1119   as a non-modifiable, competitive peptide. Negative control reactions for each inhibitor were run in

1120   the absence of Lgt enzymes (open symbols). Data are representative of at least two independent

1121   experiments each performed in triplicate.

1122

50

1123   **Figure 4: Lgti inhibit Lgt enzymatic activity in bacterial cells. (a)** Schematic representing the

1124   isolation of PAP and non-PAP fractions. Bacterial cultures were resuspended in 6 mL of PAP

1125   extraction buffer and centrifuged at 100,000 × g for 60 minutes. 6 mL of supernatants were

1126   collected and pellets were resuspended in 200 μL of PAP extraction buffer. PG-linked Lpp forms

1127   were more readily detected with the concentrated PAP fractions. **(b)** SDS fractionation of WT

1128   CFT073 cells to distinguish PG-associated versus non-PG-associated forms of Lpp.

1129   CFT073*imp4213* cells were treated with SDS to enrich for PAP and non-PAP fractions as discussed

1130   in the Methods and Western blot analysis was performed to detect levels of Lpp. GroEL was used

1131   as a control for enrichment of the PAP fraction. While triacylated free Lpp (*) is enriched in the

1132   SDS-soluble non-PAP fraction, higher molecular weight Lpp species (§, †) are enriched in the SDS-

1133   insoluble PAP fraction (§ = PG-linked diacylglyceryl pro-Lpp, DGPLP; † = other PG-linked Lpp

1134   forms). Molecular weight markers (kDa) are denoted on the left of the blots. **(c)** Detection of Lpp

1135   intermediates in MG1655Δ*lgt*, MG1655Δ*lspA* and MG1655Δ*lolCDE* inducible deletion strains by

1136   Western blot analysis. WT or inducible deletion strains were treated with 2% arabinose (A) or

1137   0.2% glucose (G) and total cell lysates were harvested at 3 hours post treatment (Ø = unmodified

1138   pro-Lpp, UPLP). PG-linked DGPLP (§) and other higher molecular weight Lpp species (†)

1139   accumulated after LspA depletion. **(d)** Accumulation of pro-Lpp in cells treated with Lgti.

1140   CFT073*imp4213* cells expressing an arabinose inducible form of Lpp (*CFT073imp*4213Δ*lpp:lpp*^{Ara})

1141   were incubated with arabinose for 30 minutes prior to treatment with 0.5×MIC concentrations of the

1142   inhibitors for another 30 minutes. Lpp forms are denoted as described above. **(e)** Lgti treatment

1143   leads to cell morphology changes and membrane blebs. CFT073*imp4213* cells were left untreated

1144   or treated with Lgti at 1×MIC for 30 minutes, fixed and incubated with FM-64 dye (red) and DAPI

1145   solution (blue) to stain membranes and nucleic acid, respectively, and visualized by confocal

51

1146   microscopy. Arrows represent membrane blebs and scale bars represent 3 μm. **(f)** Quantitation of

1147   cell size after treatment Lgti. A total of 104 ± 4 cells per treatment were quantitated using ImageJ

1148   (*p = 0.04; ***p = 0.002). **(g)** CRISPRi knock-down of *lgt* gene expression sensitizes cells to Lgti

1149   but not LspAi and LolCDEi. *E. coli* BW25113 cells expressing dCas9 and gRNAs specific to *lgt*,

1150   *lspA* or *lolC* were untreated (black bars) or treated (white bars) with 2 μM Lgti (G2823 and G2824),

1151   0.05 μM LspAi (globomycin) or 0.8 μM LolCDEi (C1). A scrambled (scr) gRNA and gRNA

1152   specific to *folA* (dihydrofolate reductase) were used as negative controls. Bacterial growth was

1153   measured by OD_{600} and values were normalized to the untreated sample for each gRNA, which was

1154   set at 100% (***p < 0.001). Data are representative of at least two independent experiments each

1155   performed in triplicate.

1156

1157   **Figure 5: *lpp* deletion does not rescue growth after Lgti treatment.** CFT073*imp*4213 (black),

1158   CFT073*imp*4213Δ*lpp* (blue) or CFT073*imp*4213Δ*lpp* complemented with pBAD24 plasmids

1159   encoding WT *lpp* (red) or *lpp*Δ*K* (green) were untreated (filled symbols) or treated (open symbols)

1160   with 12.5 μM Lgti G2824 **(a)**, 3.2 μM LspAi (GBM) **(b)**, 6.3 μM LolCDEi (C1) **(c)** and 1.6 μM

1161   vancomycin **(d)**. G2823 was not be tested due to limitations in compound availability. CFUs were

1162   enumerated at various times post treatment. **(e)** CFT073*imp*4213, CFT073*imp*4213Δ*lpp* or

1163   CFT073*imp*4213Δ*lpp* complemented with WT *lpp* or *lpp*Δ*K* were treated with SDS to enrich for

1164   PAP and non-PAP fractions. As the PAP fraction is 30-fold more concentrated than the non-PAP

1165   fraction, it is more appropriate to compare different mutants within the same fraction. Lpp forms

1166   are denoted as previously described (* = Triacylated free Lpp; § = PG-linked DGPLP; ø = UPLP; †

1167   = other PG-linked Lpp forms; Δ = putative Lpp dimer). The identity of the band in Figure 5e

1168   below the putative Lpp dimer (Δ) is unknown and could represent a degradation product. The

1169   LppΔK is his-tagged and hence migrates slower on SDS-PAGE relative to the mature triacylated

1170   Lpp. Data are representative of three independent experiments. **(f)** Lgt depletion leads to loss of

1171   PG-linked Lpp and Pal. CFT073Δ*lgt* inducible deletion cells were grown in arabinose (Ara) or

1172   glucose (Glu) and Lpp and Pal expression was determined in total cell lysates (TL), SDS-insoluble

1173   (PAP) and SDS-soluble (non-PAP) fractions at 3 and 5 hours post treatment. GroEL was used as a

1174   control for fractionation. Lpp forms are denoted by symbols as described in Figure 5e. **(g)** Lgti

1175   treatment leads to loss of PG-associated Lpp and Pal. CFT073*imp*4213 cells were treated with Lgti

1176   (G2823 and G2824), LspAi (GBM) or LolCDEi (C1) for 30 minutes at 0.5×MIC and levels of Lpp

1177   and Pal were measured in total cell lysates, PAP and non-PAP fractions. Lpp forms are denoted by

1178   symbols as described above.

1179

1180   **Figure 6: Inhibition of Lgt leads to depletion of essential OM lipoproteins and OMPs and**

1181   **minimal IM accumulation of PG-linked DGPLP. (a)** CFT073*imp*4213 cells were treated with

1182   Lgti (G2823 and G2824), LspAi (GBM) or LolCDEi (C1) for 60 minutes at 1×MIC and subjected

1183   to sucrose gradient ultracentrifugation as described in the Methods. IM and OM fractions were

1184   assigned based on the expression of MsbA and OmpA, respectively. These data re representative of

1185   at least three independent experiments. **(b)** CFT073*imp*4213 cells were treated with Lgti (G2823

1186   and G2824), LspAi (GBM) or LolCDEi (C1) and IM were solubilized using sarkosyl. Lpp and Pal

1187   levels were probed using Western blot analyses. Lpp forms denoted in the figure are as follows (* =

1188   triacylated free Lpp; § = PG-linked DGPLP; ø = UPLP; † = other PG-linked Lpp forms; Δ =

1189   putative Lpp dimer). IM fractions were probed for MsbA and BamA as controls. Levels of

1190   triacylated free Lpp (*), UPLP (ø) and DGPLP (§) were quantitated by normalizing to MsbA and

1191   levels detected in untreated cells (-) were set at 1.
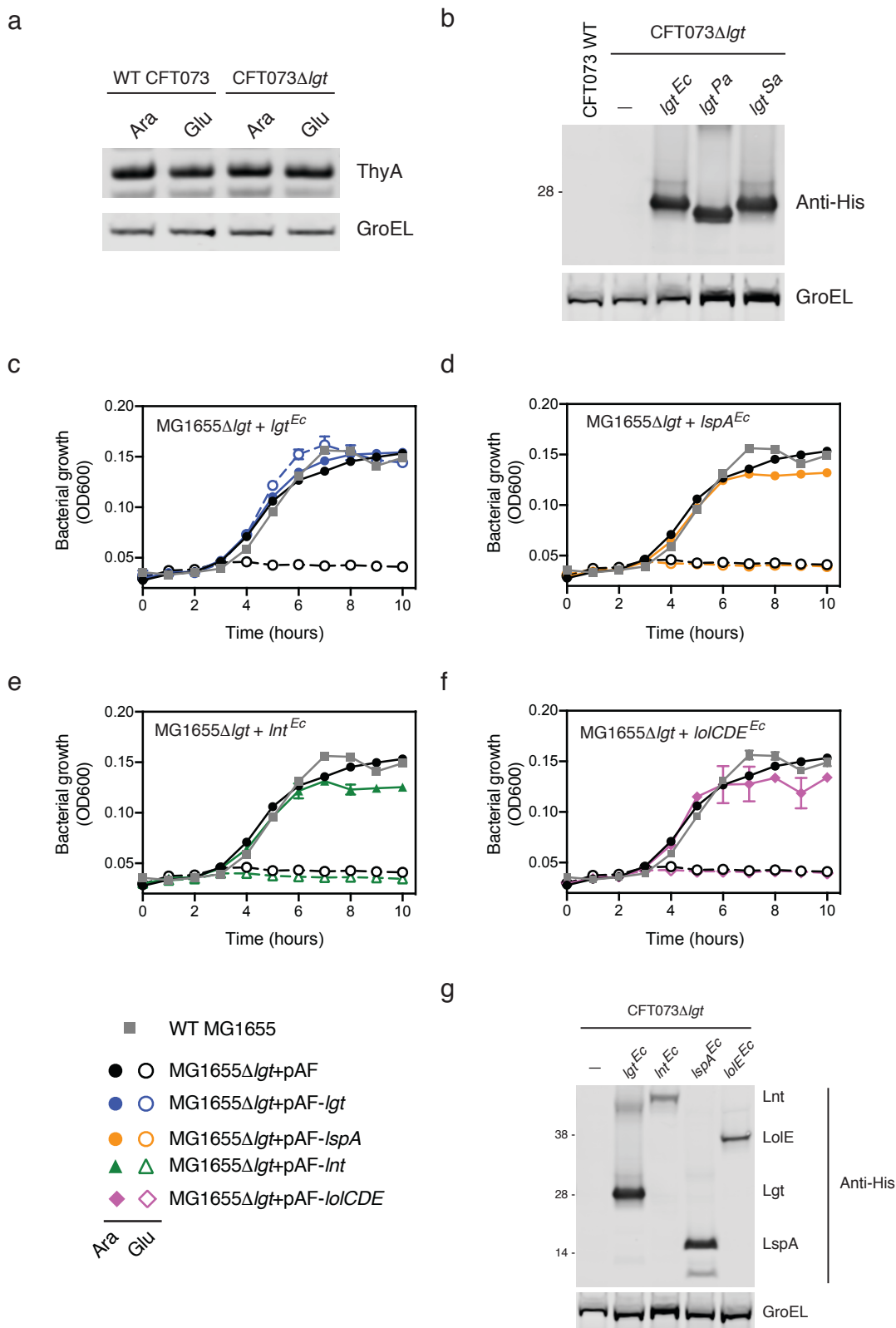
1192

1193

1194

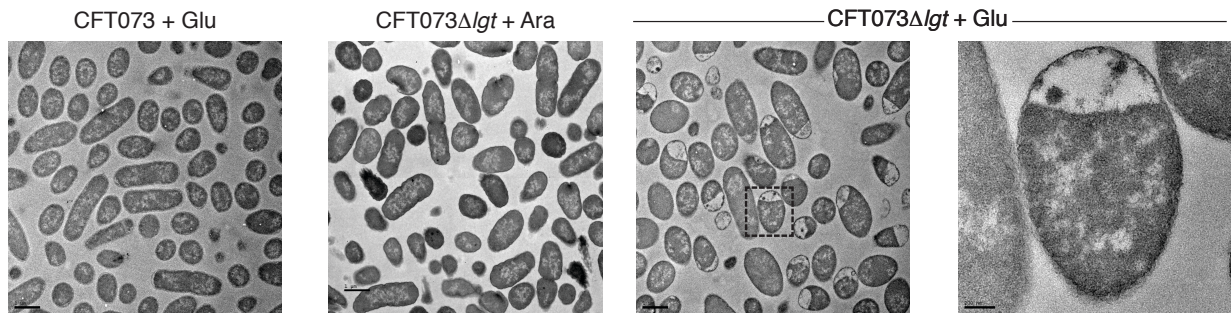1195

1196

1197

1198

1199

1200

Diao et al. Supplementary Information
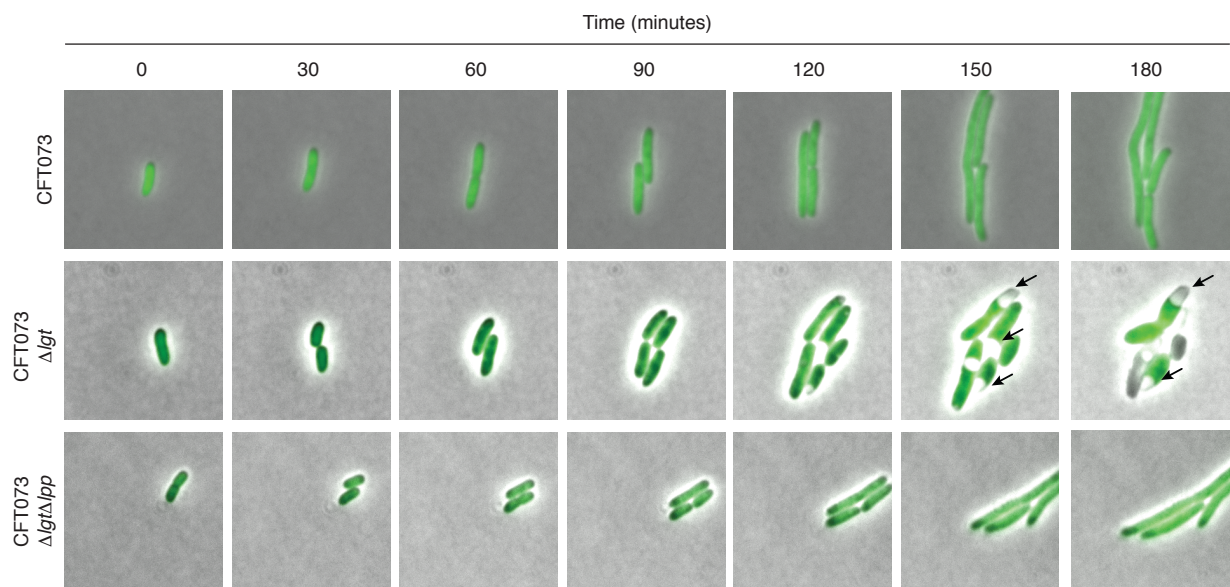
Figure 2-supplement 1

Diao et al. Supplementary Information
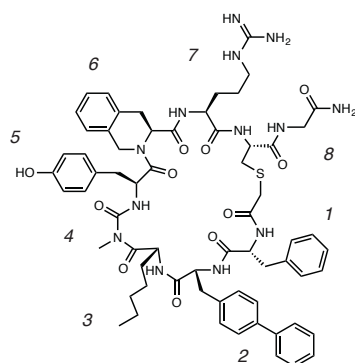
Figure 2-figure supplement 2

a

b

1
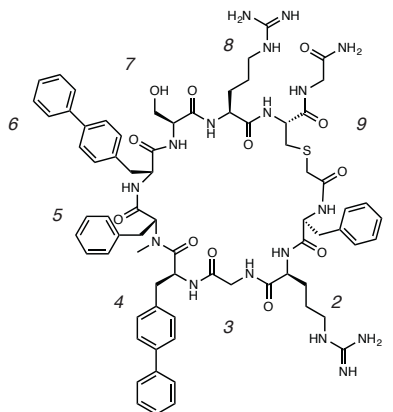
2

3

4

5

6

7

2

Diao et al. Supplementary Information

Figure 3-supplement 1
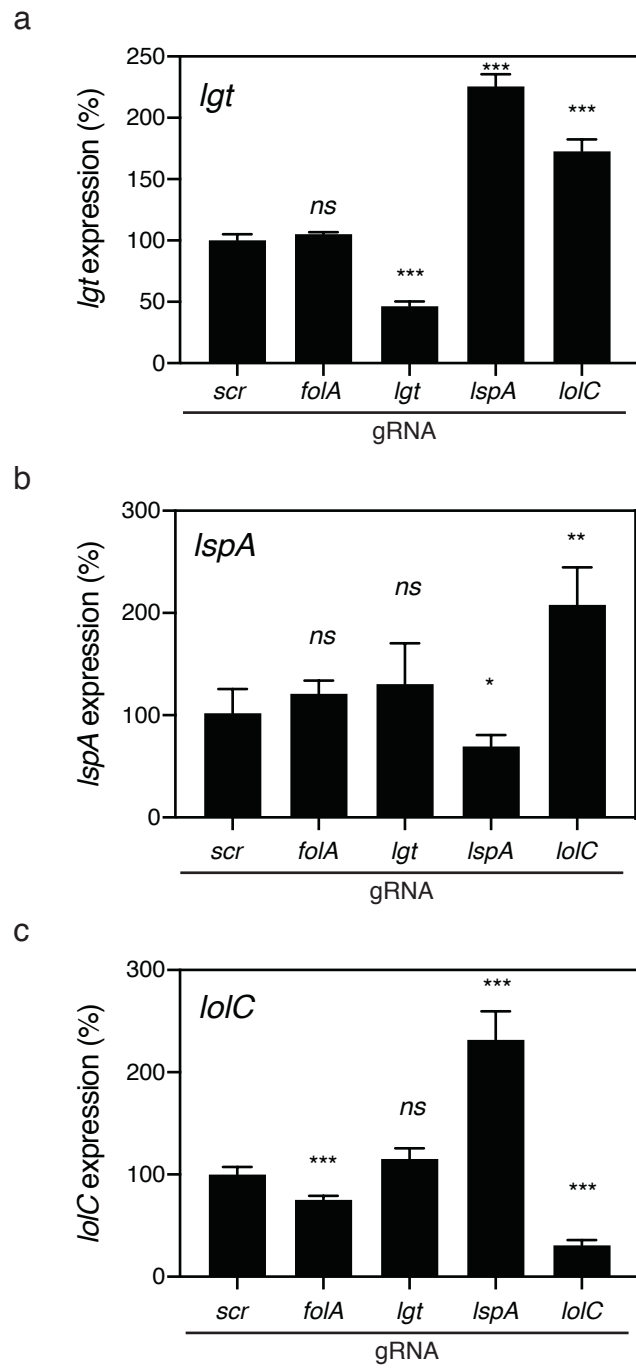

508: ClAcf-Bph-Ahp-MeG-Tyr-Tic-Arg-Cys-Gly-NH2
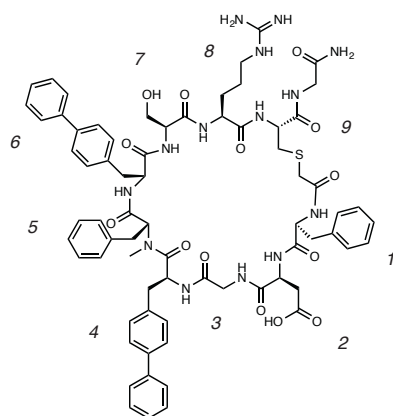
693: ClAcf-Asp-Gly-Bph-MeF-Bph-Ser-Arg-Cys-Gly-NH2

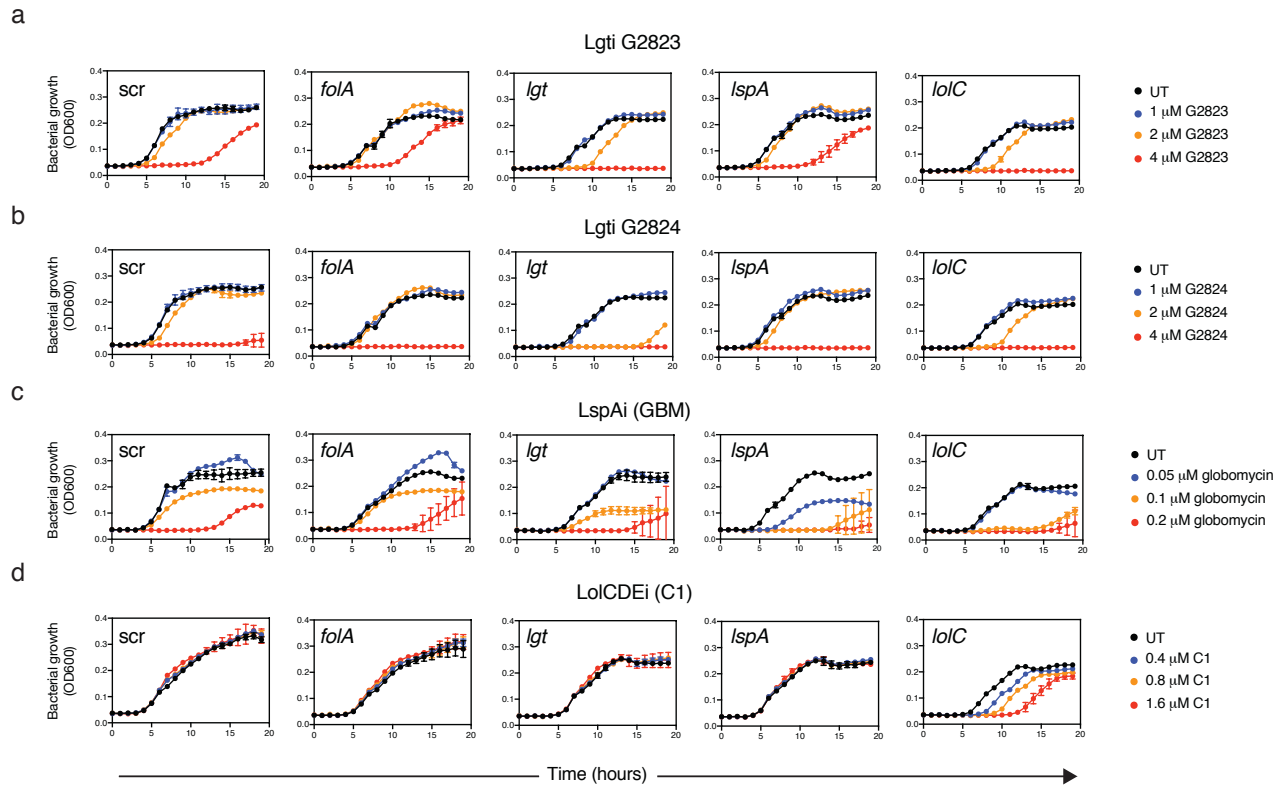

692: ClAcf-Arg-Gly-Bph-MeF-Bph-Ser-Arg-Cys-Gly-NH2

1

3

Diao et al. Supplementary Information

Figure 4-supplement 1

a

b

c

1

2

4

Diao et al. Supplementary Information

Figure 4-supplement 2
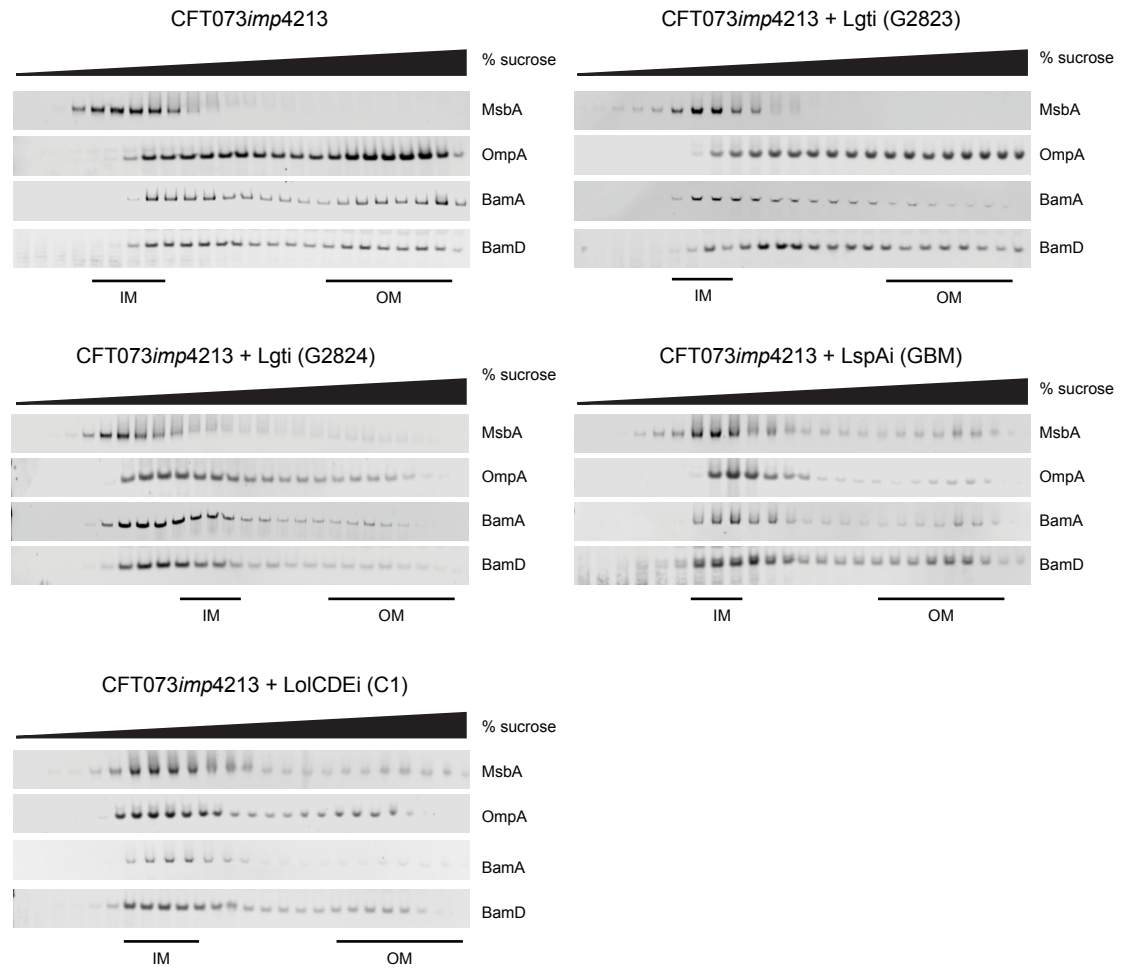
Figure 5-supplement 1
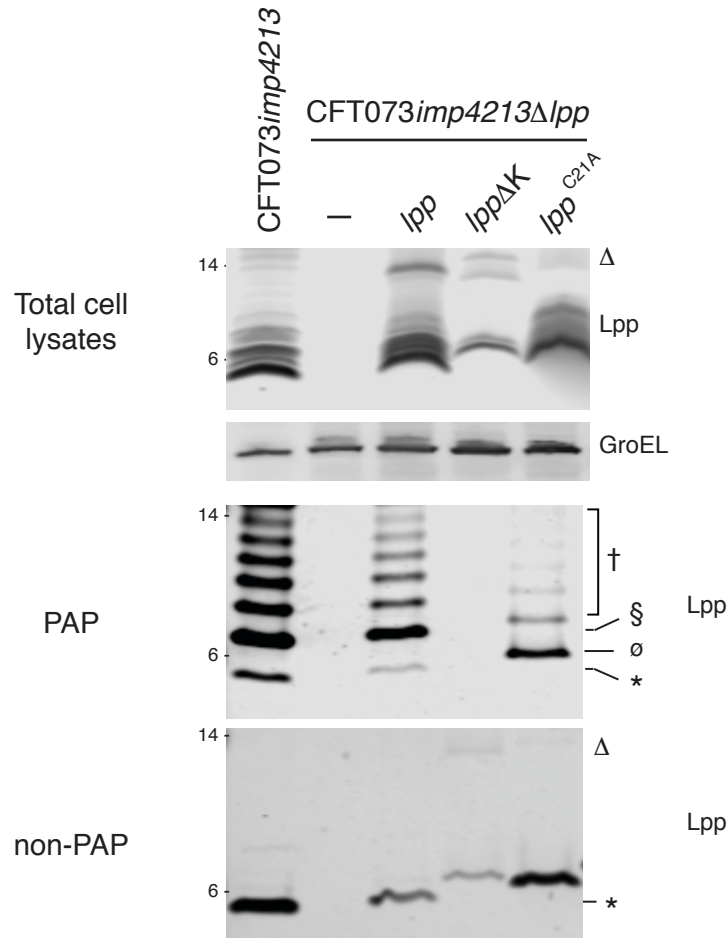
† = Other PG-linked Lpp forms
Δ = putative Lpp dimer
§ = PG-linked diacylglyceryl pro-Lpp (DGPLP)
ø = Unmodified pro-lpp (UPLP)
* = Triacylated free Lpp

1

2

3

4

Figure 6-supplement 1

Diao et al. Supplementary Information

1 **Figure supplement legends**

2 **Figure 2-figure supplement 1: (a)** Normal expression of thymidylate synthase (ThyA) after

3 depletion of Lgt. WT CFT073 and CFT073Δ*lgt* were grown under wild-type (4% arabinose, Ara)

4 or depleted (0.2% glucose, Glu) conditions for 4 hours and total cell lysates were subjected to

5 Western blot analyses using an anti-ThyA antibody. GroEL was used as a loading control. **(b)**

6 Western blot analyses confirming protein expression after complementation with pLMG18

7 expressing *lgt* from *E. coli* (*lgt*^Ec^), *P. aeruginosa* (*lgt*^Pa^) or *S. aureus* (*lgt*^Sa^). All complemented *lpp*

8 contain a c-terminal His-tag. **(c-f)** Loss of *E. coli* MG1655Δ*lgt* viability after Lgt depletion is

9 rescued after complementing with *E. coli lgt* (*lgt*^Ec^) but not *E. coli lspA* (*lspA*^Ec^), *lnt* (*lnt*^Ec^) or

10 *lolCDE* (*lolCDE*^Ec^). 2.5 mM IPTG was used to induce expression of *E. coli lspA*, *lnt* or *lolCDE*.

11 Cells were grown in arabinose (filled symbols, Ara) or glucose (open symbols, Glu) and bacterial

12 growth was measured by OD$_{600}$. **(g)** Anti-His Western blot analyses demonstrating protein

13 expression of *E. coli* Lgt, LspA, Lnt and LolE in CFT073Δ*lgt* cells complemented with His-tagged

14 versions of the respective genes.

15

16 **Figure 2-figure supplement 2:** Lgt depletion results in IM contraction and the expected globular

17 cellular phenotype. **(a)** CFT073 and CFT073Δ*lgt* deletion strains were treated for 2 hours with 4%

18 arabinose (Ara) or 0.2% glucose (Glu) and samples were processed for imaging by Transmission

19 electron microscopy. Bars represent 1 μm (200 nm for last panel). **(b)** Live cell imaging of WT

20 CFT073, CFT073Δ*lgt* and CFT073Δ*lgt*Δ*lpp* inducible deletion strains containing a plasmid

21 expressing *gfp* (pGFP) were grown in the presence of 0.2% glucose. Phase contrast and

8

1   fluorescence microscopy images were overlayed at various times post treatment. Arrows denote IM

2   contraction which is not observed in the strain containing the *lpp* deletion.

3

4   **Figure 3-figure supplement 1:** Chemical structures of original hit macrocycles **508**, **692** and **693**

5   identified in the library screen. The sequences of the macrocycles are represented in a linear format

6   using the three letter amino acid codes. Non-natural amino acids are as follows: N-α-Methyl-L-

7   phenylalanine (MeF), N-α-Methyl-L-glycine (MeG, Sarcosine), (S)-2-Aminoheptanoic acid (Ahp),

8   4-Phenyl-L-phenylalanine (Bph) and (S)-1,2,3,4-Tetrahydroisoquinoline-3-carboxylic acid (Tic).

9   CIAcf was fixed at the first position and used for cyclization.

10

11   **Figure 4-figure supplement 1:** Efficiency of CRISPRi-mediated downregulation of target genes.

12   Total RNA was harvested from *E. coli* BW25113 cells transformed with scrambled (scr) gRNA or

13   gRNA specific for *folA*, *lgt*, *lspA*, and *lolC* and gene expression of *lgt* **(a)**, *lspA* **(b)** and *lolC* **(c)** was

14   measured by RT-qPCR. Relative gene expression of *lgt*, *lspA* and *lolC* were calculated by

15   normalizing to *rpoB* levels using the $2^{-\Delta\Delta CT}$ method. Expression levels are graphed after

16   comparison to "scr" gRNA, which was set at 100%. Data are representative of two independent

17   experiments each performed in duplicate (*ns* = not significant, *p < 0.05, **p < 0.01, ***p < 0.001).

18

19   **Figure 4-figure supplement 2:** Kinetics of growth inhibition after CRISPRi gRNA induction in *E.*

20   *coli* BW25113. BW25113 cells expressing either scrambled (scr) gRNA or gRNAs specific to *folA*,

21   *lgt*, *lspA* or *lolC* were treated with **(a)** Lgti G2823, **(b)** Lgti G2824, **(c)** LspAi (GBM) and **(d)**

1 LolCDEi (C1) and bacterial growth was measured by OD_{600}. For all inhibitors, three concentrations

2 were tested based on the MIC of each molecule and compared to untreated cells (UT, black) (Lgti =

3 4, 2 and 1 µM; LspAi = 0.2, 0.1 and 0.05 µM and LolCDEi = 1.6, 0.8 and 0.4 µM). Data are

4 representative of three independent experiments each performed in triplicate.

5

6 **Figure 5-figure supplement 1:** Determination of PG-linkage of WT Lpp, LppΔK and Lpp[C21A].

7 CFT073*imp*4213, CFT073*imp*4213Δ*lpp* or CFT073*imp*4213Δ*lpp* complemented with WT *lpp*,

8 *lpp*ΔK or *lpp*[C21A] were treated with SDS to isolate PAP and non-PAP fractions. Lpp levels were

9 detected by Western blot analyses in total cell lysates, PAP and non-PAP fractions. The Lpp[C21A]

10 mutant contains an alanine in place of the conserved cysteine in the lipobox. The *lpp*ΔK construct

11 is His-tagged and hence migrates slower on SDS-PAGE. Lpp forms are denoted in the figure (* =

12 triacylated free Lpp; § = PG-linked DGPLP; ø = UPLP; † = other PG-linked Lpp forms; Δ =

13 putative Lpp dimer).

14

15 **Figure 6-figure supplement 1:** Membrane localization of BamA and BamD in CFT073*imp*4213

16 cells treated with Lgti (G2823 and G2824), LspAi (GBM) or LolCDEi (C1) for 60 minutes at

17 1×MIC and subjected to sucrose gradient ultracentrifugation as described in the Methods. Levels of

18 BamA and BamD were detected by Western blot analyses. IM and OM fractions were assigned

19 based on the expression of MsbA and OmpA, respectively, as presented in Figure 6.

20

21

Diao et al. Supplementary Information

1   **Table S1**: Lgti minimal inhibitory concentrations (MIC) against LolCDE-resistant *E. coli* isolates
2
3

MG1655*imp4213*	MIC (µM)					
	Lgti (G9066)	Lgti (G2823)	Lgti (G2824)	LspAi (GBM)	LolCDEi (C2)	Vancomycin
WT	3.1	4.7	3.1	0.2	2.4	0.8
LolC (Q258K)	6.3	3.1	3.1	0.3	75	0.8
LolC (N265K)	3.1	6.3	3.1	0.2	37.5	1.2
LolD (S43R)	6.3	4.7	3.1	0.2	37.5	0.8
LolE (F367L)	6.3	3.1	3.1	0.3	25	1.2
LolE (P372L)	3.1	6.3	3.1	0.2	50	1.2

4

5

6

7

8

9

10

11

12

13

14

15

16

17

18

19

20

21

11

Diao et al. Supplementary Information

1   **Table S2:** Bacterial strains and plasmids used in this study

Bacterial strains	Description	Reference
E. coli		
BW25113	rrnB3 DElacZ4787 hsdR514 DE(araBAD)567 DE(rhaBAD)568 rph-1	(Baba et al., 2006)
MG1655	*E. coli* K-12 F- lambda- *ilvG* negative, *rfb-50 rph-1*	ATCC 700926
MG1655Δ*lgt*	MG1655 Δ*lgt*::kan with an arabinose-inducible integrated *lgt* copy	This study
MG1655Δ*lgt*Δ*lpp*	MG1655 Δ*lpp*, Δ*lgt*::kan containing an arabinose-inducible integrated *lgt* copy	This study
MG1655Δ*lspA*	Arabinose-inducible conditional knockout of *lspA*	(Pantua et al., 2020)
MG1655Δ*lspA*Δ*lpp*	MG1655 Δ*lpp*, Δ*lspA*::kan containing an arabinose-inducible integrated *lspA* copy	This study
MG1655Δ*lolCDE*	Arabinose-inducible conditional knockout of *lolCDE*	This study
MG1655Δ*lolCDE*Δ*lpp*	MG1655 Δ*lpp*, Δ*lolCDE*::kan containing an arabinose-inducible integrated *lolCDE* copy	This study
CFT073	Bacteremia isolate, wild-type (O6:K2:H1)	ATCC 700928
CFT073Δ*lgt*	CFT073 Δ*lgt*::kan containing an arabinose-inducible integrated *lgt* copy	This study
CFT073*imp4213*	CFT073 carrying the *imp4213* allele in *lptD*	(Ho et al., 2018)
CFT073*imp4213*Δ*lgt*	CFT073 Δ*lgt*::kan containing an arabinose-inducible integrated *lgt* copy and carrying the *imp4213* allele in *lptD*	This study
CFT073*imp4213*Δ*lpp*	CFT073 Δ*lpp*::kan carrying the *imp4213* allele in *lptD*	This study
*CFT073imp*4213Δ*lpp:lpp*ᵂᵀ	*CFT073imp*4213Δ*lpp*::kan containing pBAD24 expressing *lpp*	This study
TOP10	pWQ601, general cloning strain	Invitrogen
S. aureus USA300	USA300 FPR3757	Center for Staphylococcal Research, Nebraska
A. baumannii 19606	*Acinetobacter baumannii* strain isolated in a patient urine sample	ATCC
P. aeruginosa PA14	*Pseudomonas aeruginosa* strain UCBPP-PA14 originally isolated from a burn wound	ATCC
PA14*imp*4213	*Pseudomonas aeruginosa* UCBPP-PA14 containing the imp4213 mutation in *lptD*	This study
Plasmids		
pKD4	Kanamycin resistance (KanᴿR) cassette flanked by FRT (FLP recognition target) sites, oriRγ	(Silhavy, Kahne, & Walker, 2010)
pKD46	Expresses the phage λ Red recombinase, AmpᴿR, temperature sensitive, oriRγ	(Cowles, Li, Semmelhack, Cristea, & Silhavy, 2011; Wilson & Bernstein, 2015)
pCP20	Thermal induction of FLP recombinase expression, Ampᴿ, temperature sensitive	(Kovacs-Simon, Titball, & Michell, 2011)
pLDR8	Lambda integrase expression vector	ATCC 77357
pLDR9	Lambda att site integration vector	ATCC 77358

Diao et al. Supplementary Information

pBAD24	Arabinose inducible expression vector	ATCC 87399
pBAD24-*lpp*	pBad24 expressing *E. coli lpp*	This study
pBAD24-*lppΔK*	pBad24 expressing *E. coli lppΔK*	This study
pBAD24-*lpp*C21A	pBad24 expressing *E. coli lpp*C21A	This study
pdCas9-bacteria_GNE	Based on AddGene plasmid 44249	This study
pgRNA-bacteria_GNE	Based on AddGene plasmid 44251	This study
pLMG18	Low-copy IPTG-inducible expression plasmid, CmR	(M. Tokunaga, Tokunaga, & Wu, 1982)
pLMG18-*lgt*Ec	pLMG18 expressing *E. coli lgt*	This study
pLMG18-*lgt*Sa	pLMG18 expressing *S. aureus lgt*	This study
pLMG18-*lgt*Pa	pLMG18 expressing *P. aeruginosa lgt*	This study
pLMG18-*lspA*Ec	pLMG18 expressing *E. coli lspA*	This study
pLMG18-*lnt*Ec	pLMG18 expressing *E. coli lnt*	This study
pLMG18-*lolCDE*Ec	pLMG18 expressing *E. coli lolCDE*	This study
pGFP	pBla_Short encoding sfGFP	(Storek et al., 2018)

1

References

3 Baba, T., Ara, T., Hasegawa, M., Takai, Y., Okumura, Y., Baba, M., et al. (2006). Construction of
4   Escherichia coli K-12 in-frame, single-gene knockout mutants: the Keio collection. *Molecular Systems*
5   *Biology*, 2(1), 2006.0008. http://doi.org/10.1038/msb4100050
6 Cowles, C. E., Li, Y., Semmelhack, M. F., Cristea, I. M., & Silhavy, T. J. (2011). The free and bound forms
7   of Lpp occupy distinct subcellular locations in Escherichia coli. *Molecular Microbiology*, 79(5), 1168–
8   1181. http://doi.org/10.1111/j.1365-2958.2011.07539.x
9 Ho, H., Miu, A., Alexander, M. K., Garcia, N. K., Oh, A., Zilberleyb, I., et al. (2018). Structural basis for
10   dual-mode inhibition of the ABC transporter MsbA. *Nature*, 557(7704), 196–201.
11   http://doi.org/10.1038/s41586-018-0083-5
12 Kovacs-Simon, A., Titball, R. W., & Michell, S. L. (2011). Lipoproteins of bacterial pathogens. *Infection*
13   *and Immunity*, 79(2), 548–561. http://doi.org/10.1128/IAI.00682-10
14 Pantua, H., Skippington, E., Braun, M.-G., Noland, C. L., Diao, J., Peng, Y., et al. (2020). Unstable
15   Mechanisms of Resistance to Inhibitors of Escherichia coli Lipoprotein Signal Peptidase. *mBio*, 11(5),
16   VMBF–0016–2015. http://doi.org/10.1128/mBio.02018-20
17 Silhavy, T. J., Kahne, D., & Walker, S. (2010). The bacterial cell envelope. *Cold Spring Harbor Perspectives*
18   *in Biology*, 2(5), a000414–a000414. http://doi.org/10.1101/cshperspect.a000414
19 Storek, K. M., Auerbach, M. R., Shi, H., Garcia, N. K., Sun, D., Nickerson, N. N., et al. (2018). Monoclonal
20   antibody targeting the β-barrel assembly machine of Escherichia coli is bactericidal. *Proceedings of the*
21   *National Academy of Sciences of the United States of America*, 115(14), 3692–3697.
22   http://doi.org/10.1073/pnas.1800043115
23 Tokunaga, M., Tokunaga, H., & Wu, H. C. (1982). Post-translational modification and processing of
24   Escherichia coli prolipoprotein in vitro. *Proceedings of the National Academy of Sciences of the United*
25   *States of America*, 79(7), 2255–2259. http://doi.org/10.1073/pnas.79.7.2255
26 Wilson, M. M., & Bernstein, H. D. (2015). Surface-Exposed Lipoproteins: An Emerging Secretion
27   Phenomenon in Gram-Negative Bacteria. *Trends in Microbiology*.
28   http://doi.org/10.1016/j.tim.2015.11.006

29

30

Diao et al. Supplementary Information

1   **Table S3:** Primers used in this study for strain generation and quantitative PCR

Primer	Sequence (5' to 3')
Strain generation	
CFT073Δ*lgt*.F	TTTCAATCGCTGTTCTCTTTCAGCGAAATAACAAGAACTTGTGGTGACAGGTGTAGGCTGGAGCTGCTTC
CFT073Δ*lgt*.R	CCTTCGTCGAGCACTTTTTGCATCAGTTCTAAATACTGTTTCATGGTTCCCATATGAATATCCTCCTTAGTTCCTATTC
MG1655Δ*lolCDE*.F	CGGGGGCTTTTCAGATTAGCCCTGACGATCACTTACAGTTCAGACGTTTACCCATCTTGCTTTCGCTTATATACTCGTGTCTTTGCTACAGCAACCAGACGGATTTCGTGTAGGCTGGAGCTGCTTC
MG1655Δ*lolCDE*.R	CCCACTGCAACTGCCGACCGCTATCAAACACGCCAAGCGCAATTTTTGTTCCACCAATATCAAACCCGTAATACATTGCCGCTCCTTGTTTTAATGTACTGCCCATATGAATATCCTCCTTAGTTCCTATTC
Quantitative PCR	
lgt.F	CTCGGTGGACGTATTGGTTATG
lgt.R	TCACCACGATAACGCCAATC
lgt.PRB	/ _56-FAM_ / ACAATTTCC /ZEN/ CGCAGTTTATGGCCG / _3IABkFQ_ /
lspA.F	TCGATCTGGGCAGCAAATAC
lspA.R	CGCTATCGGCAAGGAAACTAA
lspA.PRB	/ _56-FAM_ / TGCAGATTA /ZEN/ AGCGACGGGAACAGC / _3IABkFQ_ /
lolC. F	CCACAGGCAATTCTCTCTTCT
lolC.R	TAGGTGCGACGCGATTAAC
lolC.PRB	/ _56-FAM_ / CTCTCTTAA /ZEN/ CCCGCAGCAACTCCC / _3IABkFQ_ /

2
3

14